A protein kinase A-regulated centrosomal actin pool sets the threshold for T cell polarization

Morgane Simao #, Fabienne Régnier # & Clotilde Randriamampita*

Université Paris Cité, CNRS, Inserm, Institut Cochin, F-75014 Paris, France

# MS and FR equally contributed to this work
* Corresponding author

Abstract

T lymphocyte migration triggered by chemokine stimulation is preceded by cell polarization. The acquisition of this asymmetry requires a profound cell rearrangement, particularly of the cytoskeleton. The mechanism by which a uniform signal triggered by chemokine receptors rapidly leads to this asymmetry is largely elusive. Using cell imaging, we emphasize that the centrosome dictates the position of the polarization axis in T lymphocytes. Mechanistically, we highlight that the T cell shape is controlled by the amount of actin filaments surrounding the centrosome. In resting conditions as well as after chemokine stimulation, the activity of a specific pool of protein kinase A regulates this cytoskeleton compartment. Once the centrosomal actin is reduced below a certain threshold, the symmetry breaking is catalyzed. This study points to a critical protein kinase A signaling pathway in the establishment of the immune response.

Introduction

T lymphocyte migration constitutes a key step of the immune response considering that allows the cells to explore primary lymphoid organs as well as tissue. It is conditioned by physical and chemical microenvironment (Krummel et al, 2016) and is thus a result of a combination of 3D confinement, durotaxis, topotaxis, chemotaxis, haptotaxis, etc… which may deliver opposite guidance cues (Shellard & Mayor, 2020), (Kameritsch & Renkawitz, 2020). Chemical signals are in particular due to bound or soluble chemokines (CXCL12, CCL19 and CCL21). T cell stimulation by chemokine triggers a major rearrangement of the cell compartments (organelles, cytoskeleton, …) (Pineau et al, 2023) that leads to an asymmetrical cellular organization with two main structures: the lamellipodium at the front and the uropod at the back. This cell polarization is an absolute prerequisite for the cell to migrate and requires important remodeling of the cytoskeleton. In particular, chemokine triggers an increase of actin polymerization which progressively accumulates at the cell front, conferring a highly dynamic lamellipodium (Real et al, 2007). The uropod at the cell back is surrounded by an actomyosin network whose contraction facilitates T cell migration. The establishment of this polarization axis takes place within a few minutes after chemokine stimulation. Chemokine receptor activation has been reported to trigger several signaling pathways, such as calcium signaling, ERK, PI3 kinase activation, small GTPases activation or cAMP modulation (Kehrl, 2006), (Thelen & Stein, 2008). Although these different elements seem to be important for T cell polarization and/or migration (Niggli, 2014), their importance in the initiation of polarization i.e in early (seconds-minutes) steps leading to the establishment of the asymmetric distribution of cellular components and polarity regulators, is still unclear (Mastrogiovanni et al, 2022).

T cell polarization appears in two important immune functions: upon immune synapse formation and after chemokine stimulation. In the first case, stimulation takes place at a specific location imposed by the point of contact with the antigen presenting cell where a signaling pole is formed locally. The position of the polarization axis is then driven by the site of stimulation. Conversely, upon chemokine addition, the initial stimulation might be homogeneous or heterogeneous (gradient of soluble or

46 bound chemokine). However, in both cases, it rapidly triggers a symmetry breaking which allows the
47 cell to polarize in one clear direction after a couple of minutes. One could therefore wonder whether,
48 after a uniform stimulation, the orientation of this axis takes place randomly, or whether it is
49 imposed by an intrinsic cellular factor. In other words, is it possible in that case, to predict in which
50 direction a cell will polarize after uniform chemokine stimulation?
51 Among the intrinsic cellular factors which could condition the position of the polarization axis,
52 various hypothesis can be considered. An uneven distribution of chemokine receptors at the cell
53 surface might lead to the formation of several local signaling poles. The pole with the highest
54 receptor density might force the development of the polarization axis at a specific place. A
55 heterogeneous distribution of polymerized actin or of factors promoting this process, could also
56 favor the formation of the lamellipodium in a specific position after chemokine stimulation. Finally,
57 the centrosome, a single-copy organelle, is now clearly considered not only as a microtubule-
58 organizing center (MTOC) but also as a signaling platform (Langlois-Lemay & D'Amours, 2022) which
59 may consequently transform a uniform external signal into a local response. As a non-membrane
60 organelle, the centrosome is surrounded by a pericentriolar material linked to the cytoskeleton. A
61 large number of proteins are indeed associated with this structure, including protein kinases and
62 phosphatases (Schatten, 2008). It is involved in several cellular processes (Elric & Etienne-
63 Manneville, 2014), in particular in the positioning of subcellular structures upon immune synapse
64 formation (Kloc et al, 2014).
65 Recently, the centrosome has been reported to not only be a microtubule, but also an actin
66 organizing center (Farina et al, 2015). In T and B lymphocytes, a decrease in the pool of polymerized
67 actin that surrounds the centrosome has been reported upon immune synapse formation (Obino et
68 al, 2016), (Cassioli et al, 2021), (Ibanez-Vega et al, 2019), (Bello-Gamboa et al, 2020). Furthermore, a
69 recent study demonstrates that this pool of actin could constitute a size-dependent diffusion barrier
70 around the centrosome (Cheng et al, 2022), suggesting that any event leading to actin
71 depolymerization at this point, could induce a modification of the pericentriolar composition.

72 Interestingly, this is what is observed in B lymphocytes, where the nature of the proteins associated
73 with the centrosome is modified upon immune synapse formation (Farina et al, 2015).
74 The aim of this study is to understand whether, after uniform chemokine stimulation, the symmetry
75 break that drives the position of the polarity axis is established in a particular direction with respect
76 to the intracellular compartments or whether this is completely random. Using a combination of
77 imaging and pharmacological perturbations, we identify, in CEM T cell line as well as in human
78 primary T cells, the early signaling pathways which control this event and show that a specific pool of
79 PKA is able to control T cell polarization by regulating the level of actin around the centrosome.
80

Results

CXCL12-stimulated T cells polarize along an axis correlated with the centrosome position

T cell stimulation by chemokine triggers a very rapid cell deformation that precedes polarization itself as previously reported (Real et al, 2007). This deformation can be quantified by the cell roundness parameter which allows us to calculate how close to a circle the cell is. While the cell roundness is equal to 1 for a perfectly round cell, it decreases as long as the cell deforms. As shown on Figure 1a, unstimulated CEM T cells deposited on VCAM-1-coated coverslips present a resting roundness of around 0.85 independently of the duration of adhesion. Conversely, when the coverslips are coated with VCAM-1 plus CXCL12, the cells progressively deform. In this case, the cell stimulation can take place asynchronously depending on the time a given cell enters into contact with the CXCL12-coated coverslip. The kinetics of cell deformation can therefore be more precisely assessed by dynamic cell imaging when cells deposited on VCAM-1 coated coverslips, are stimulated at the same time by the external addition of CXCL12. As depicted in Figure 1b, in this configuration, we observed that CEM deformation starts rapidly after stimulation with a mean delay between cell stimulation and initiation of cell deformation of 112 ± 10 s (n=48 cells). As we have previously shown (Simao et al, 2021), cell polarization corresponds to a major actin cytoskeleton reorganization with an accumulation of newly polymerized actin at the front (lamellipodium), while the stable actin network becomes restricted to the cell back (uropod). This actin reorganization settles the polarization axis. We next considered whether the acquisition of this polarization axis takes place in any direction or along a predetermined position.

The centrosome, which we visualized by transfecting the cells with centrin1-GFP construct, can be used as a reference for determining the position of the polarization axis. We followed the establishment of this axis by determining the point where the cortical actin cage (labeled with SiR-Actin as previously shown (Simao et al, 2021)) opens, allowing the formation of the future lamellipodium. In the example presented in Figure 1c, it clearly appears that this event takes place in the vicinity of the centrosome. As depicted on the scheme presented in Figure 1d, we quantified this

107 observation by measuring the angle formed between the two lines [Center of the cell - Center of the
108 opening of cortical actin cage] and [Center of the cell - Centrosome]. An angle of 0° would mean that
109 the lamellipodium forms exactly in front of the centrosome. Angles distribution presents a mean
110 value of 59.7° ± 6.6 (n=60 cells from 11 independent experiments) with a median of 37.5° (Figure 1d),
111 meaning that the opening of the cortical actin cage preferentially takes place close to the
112 centrosome.
113 We then investigated the distribution of the chemokine receptors CXCR4 on unstimulated CEM T
114 cells to determine whether they display an accumulation near the centrosome. Such a
115 heterogeneous distribution could indeed trigger a local signaling pole and therefore impose the
116 position of the polarization axis at this place. However, as observed in the different cells presented in
117 Figure Supp 1a, CXCR4 labelling, although not uniform, does not present a systematic enrichment at
118 the centrosome pole. In CXCL12-activated cells, the receptors clearly accumulate at the cell front
119 (Figure Supp 1b). CXCR4 distribution can therefore not explain the preferential position of the
120 polarization axis we observe.
121
122 **Protein Kinase A activation triggered by CXCL12 stimulation is essential for cell polarization**
123 We next focused on the signaling pathways triggered during early polarity establishment, in
124 particular the cAMP, PKA and calcium (Ca) pathways. By using the FRET-based cAMP biosensor
125 TEpacVV (Klarenbeek et al, 2015) and dynamic cell imaging, we analyzed the variations of cAMP after
126 CXCL12 addition. Surprisingly, despite a supposed coupling of CXCR4 to Gi proteins, we observed a
127 very rapid rise in cAMP that reaches its maximum within a few seconds (Figure 2a). Because,
128 chemokine stimulation is known to induce a Ca increase through Gβγ-activated phospholipase C
129 (Thelen & Stein, 2008), we wondered whether Ca could be responsible for the cAMP increase
130 through a well-described Ca-cAMP crosstalk (Arige & Yule, 2022). To answer this question, we
131 simultaneously measured Ca and cAMP variations in individual CEM T cells. As shown on the
132 averaged traces presented in Figure Supp 2a, cAMP increases more slowly than Ca after CXCL12

133 addition. These results suggest that the CXCL12-induced Ca rise preceded the cAMP increase. In
134 order to directly test the causal link between the two events, the sensitivity of the cAMP increase to
135 the Ca chelator BAPTA was investigated. As shown in Figure Supp 2b, the CXCL12-induced cAMP rise
136 is significantly reduced when Ca is buffered, suggesting that the elevation of cAMP is a consequence
137 of the previous Ca increase.
138 We next investigated the consequences of the cAMP rise by measuring the variations of PKA activity
139 using the PKA biosensor exRaiAKAR2 (Zhang et al, 2020). As shown in Figure 2b, an increase in PKA
140 activity is rapidly measured after CXCL12 addition. Analysis of cAMP and PKA responses in a large
141 number of cells, reveals that cAMP levels start to increase 17.63 ± 0.63 s (n=139 cells) after CXCL12
142 addition while PKA activity rises significantly later (23.33 ± 0.75 s, n=201 cells) for (Figure 2c),
143 suggesting not surprisingly, that cAMP increase precedes PKA activation.
144 Using dynamic cell imaging, we were able to establish that cAMP increase as well as PKA activation
145 take place before the cells start to deform as shown in the examples presented in Figure 3a. This
146 observation can be quantified in single cells by measuring PKA activity simultaneously with
147 roundness evolution over time. It clearly appears that while PKA is rapidly activated, cells deformed
148 more slowly and with a certain delay, as shown in the example presented in Figure 3b. This delay is
149 72.3 ± 9.0 s (n=30 cells). These results demonstrate that CXCL12 triggers first a cAMP rise, followed
150 by an activation of PKA which itself precedes CEM T cell deformation.
151 The causal link between these events was directly investigated by testing whether PKA activation was
152 necessary for the establishment of cell polarization. For this purpose, we used H89 as an inhibitor of
153 PKA. This drug is a competitive inhibitor of ATP on kinases catalytic site, in particular that of PKA
154 although a limited number of other kinases can also be affected at the low H89 concentration we
155 used (Davies et al, 2000), (Murray, 2008). As shown in Figure 3c and on the example presented in
156 Figure Supp 2c, H89 prevents CXCL12-induced cell deformation. Interestingly, the roundness of
157 unstimulated cells is also increased with this drug, suggesting that resting PKA activity also controls
158 the shape of unstimulated cells. To complete this result, we performed some experiments on human

159 primary blood T lymphocytes (PBT). In the same way as observed with the CEM T cell line, the
160 deformation of PBT induced by the chemokine CXCL12 is also abolished by H89 pretreatment (Fig
161 Supp 3a & b). However, one can note that with these primary T cells, H89 only slightly (and
162 insignificantly) increases the resting rounding. It is probably due to the fact that resting PBT are
163 already very round. They indeed display a resting roundness statistically superior to that of CEM
164 (0.90 ± 0.01 mean of 4 experiments for PBT *vs* 0.83 ± 0.01 mean of 6 experiments for CEM).
165 To analyze the consequences on T cell behavior of H89-induced inhibition of deformation, we
166 quantified the migration by Transwell assay. As displayed in Figure Supp 3b, after 2h, CXCL12 triggers
167 the migration of 31 ± 7 % (n=3) of CEM T cells through 5µm pores. In the presence of H89, a 60 ± 1 %
168 inhibition (n=3) of cell migration was observed, demonstrating that the inhibition of CXCL12-induced
169 cell deformation results in a reduced cell migration.
170 Finally, to confirm the involvement of PKA in this process, we used another family of PKA inhibitors:
171 the cAMP analog Rp-8-CPT-cAMPS, a competitive inhibitor of PKA which binds to the cAMP binding
172 site of the regulatory subunit. Unlike H89, Rp-8-CPT-cAMPS display a high specific inhibition toward
173 PKA (Gjertsen et al, 1995). As shown in Figure Supp 5a, a similar increase in resting roundness is
174 observed when the cells are incubated with this inhibitor. However, this inhibitor is not efficient
175 enough to block the deformation induced by chemokine (Figure Supp 5a) unless the strength of the
176 stimulation is reduced by a factor 3 (Figure 2g). It suggests that, in our conditions, this inhibitor is
177 only able to counteract mild activation of PKA. Nevertheless, this result confirms the central role of
178 PKA in CXCL12-induced cell deformation.
179
180 **Upon CXCL12 stimulation, centrosomal F-actin decreases through a PKA-dependent mechanism.**
181 We then wondered what the link might be between the centrosome associated with the position of
182 the polarization axis (Figure 1d) and the protein kinase A which is required for deformation (Figure
183 2). During the last few years, several papers have reported that, upon immune synapse formation
184 (another example of T cell polarization), important remodeling takes place around T or B cell

185 centrosomes (Obino et al, 2016), (Cassioli et al, 2021), (Ibanez-Vega et al, 2019), (Bello-Gamboa et al,
186 2020). More precisely, a decrease of the F-actin content in this region has been reported. We
187 therefore studied this particular actin pool over chemokine-induced polarization.
188 In order to follow the quantity of F-actin around the centrosome upon CXCL12 stimulation, we
189 measured over time, the intensity of the phalloidin labelling in 3µm diameter area of centered on the
190 centrosome whose position is determined by pericentrin labeling (Figure 3a, insert). The kinetics
191 highlight that centrosomal F-actin rapidly decreases after CXCL12 addition (Figure 3a and example in
192 Figure 3b) reaching a minimum already around 3 minutes. To investigate whether this event depends
193 on PKA activity, we performed the same kind of experiment but in the presence of the PKA inhibitor
194 H89. In the presence of H89, F-Actin content in the centrosomal zone decreases less after CXCL12
195 addition, compared to control cells (Figure 3c). Indeed, even after 5 minute stimulation, centrosomal
196 F-actin is still above the level measured in unstimulated control cells (dashed line). Furthermore and
197 interestingly, in these conditions, the level of centrosomal F-Actin in unstimulated cells is
198 dramatically increased by a factor of 2.29 ± 0.39 (n=8 independent experiments) (Figure 3b & c).
199 Similarly to what is observed with the CEM T cell line, CXCL12 stimulation in PBT triggers a decrease
200 of centrosomal actin which is abolished under PKA inhibition by H89 (Figure Supp 4c & d).
201 Furthermore, as noticed in CEM T cells, the resting level of centrosomal actin is also strongly
202 enhanced by this inhibitor in PBT.
203 An effect similar to H89 was observed when PKA was inhibited with the specific PKA inhibitor, Rp-
204 8CPT-cAMPS. An increase of centrosomal actin is observed in unstimulated cells incubated with this
205 inhibitor. After CXCL12 stimulation, the decrease of centrosomal actin level is abolished but, like for
206 cell roundness, only if the intensity of the stimulation is reduced (Figure 3d & Supp 5b).
207 In order to have better kinetic resolution, by dynamic imaging, we measured the centrosomal F-Actin
208 decay in single CEM T cell expressing the polymerized actin reporter, LifeAct. In this configuration,
209 CXCL12 drives a very rapid F-actin decrease immediately after CXCL12 addition (Figure 3e).
210 Interestingly, H89 on its own, is able to induce a rapid increase in F-Actin, suggesting once again that,

211 even in resting cells, basal PKA activity actively controls the level of F actin content at the
212 centrosome.
213 Inspired by the results obtained upon immune synapse formation in B cells (Obino et al, 2016), where
214 the decrease of centrosomal F-actin seems to be driven by a decrease in Arp2/3 content in this area,
215 we measured in individual cells, the Arp2 content together with F-actin in the centrosomal zone in
216 control condition, after CXCL12 stimulation or in the presence of H89 (example in Figure Supp 6a).
217 Clearly, Arp2 presents a similar evolution to F-Actin: it is decreased after 5 minute CXCL12
218 stimulation while it is increased by H89 treatment (Figure Supp 6b).
219
220 **Centrosomal F-Actin is controlled by a specific pool of PKA**
221 Altogether, these results show that PKA is able to regulate the pool of centrosomal actin in resting
222 cells, as well as after CXCL12 stimulation. One could then wonder whether the PKA activity
223 responsible for this effect is equally distributed in the cell, or restricted to this specific region. By
224 measuring PKA activity through dynamic cell imaging, we sometimes but not systematically observed
225 some hot spots of activity around the centrosome. The variability of this observation might be due to
226 the low frequency of acquisition (one measurement every 10 sec). In cells, PKA activity might be
227 compartmentalized at specific intracellular locations through the family of scaffold proteins AKAP (A-
228 Kinase anchoring protein). One specific AKAP, AKAP9 (also called AKAP450, AKAP350 or CG-NAP) has
229 been reported to accumulate at the centrosome and, interestingly, to be required for T cell migration
230 (El Din El Homasany et al, 2005), (Ong et al, 2018). As shown in the example (Figure 4a), in CEM T
231 cells, AKAP450 is present and colocalizes with pericentrin, as attested by the value of the Pearson
232 coefficient (0.78 ± 0.01 n=37 cells). AKAP450 is a type II AKAP i.e. it is able to bind RII subunits of PKA.
233 To determine whether this AKAP enable compartmentalization of the PKA activity responsible for
234 centrosomal F-actin regulation, we used Ht31. This peptide is able to specifically counteract the
235 binding of type II PKA to AKAP and thus prevents compartmentalization of this class of PKA,
236 especially those bound to AKAP450. To test the efficacy of this inhibitor, we compared the

237 distribution of PKA using an antibody directed against the catalytic subunit, in the presence of the
238 inhibitory peptide (Ht31) or of the control peptide (Ht31-P). As displayed on the examples presented
239 in Fig Supp 7a, an enrichment of PKA in the centrosomal area was observed in control conditions
240 (Ht31-P), while a more homogeneous labeling within the cytoplasm was detected in the presence of
241 Ht31. This difference was quantified by calculating the ratio between the PKA intensities measured in
242 a 3µm diameter zone centered at the centrosome with one in the cytoplasm. A ratio >1 indicates an
243 accumulation of PKA at the centrosomal area. As shown in Fig Supp 7b, this ratio is a little superior to
244 1 in control conditions but is statistically reduced in the presence of the Ht31 inhibitor. These results
245 suggest there is some accumulation of PKA around the centrosome which can be reduced by Ht31.
246 We then tested the consequences of this inhibitor on CXCL12 response. As shown in Figure 4b left,
247 incubation of the cells with this peptide induces an increase of resting roundness and prevents
248 CXCL12-induced cell deformation unlike the control peptide (Ht31-P). Furthermore, in the presence
249 of this inhibitor, centrosomal F-actin still remains above the level of control cells even after CXCL12
250 stimulation (Figure 4b right). Finally, similarly to what is observed with PKA inhibitors, Ht31 induces a
251 major increase of F-Actin content at the centrosome in unstimulated cells as clearly seen in the
252 examples presented in Figure Supp 7a. Altogether, these results suggest that in resting cells, as well
253 as in CXCL12-stimulated ones, a pool of PKA anchored at the centrosome, controls the cell roundness
254 and the quantity of centrosomal F-actin.
255
256 **Centrosomal F-actin decrease is accompanied by an increase in centrosomal microtubules**

257 We then wondered what could be the consequences of the decrease of F-actin at the centrosome.
258 Among the different possibilities, one can hypothesize that centrosomal actin decrease permits an
259 increase of microtubule polymerization at this location as previously reported (Inoue et al, 2019). We
260 then quantified the two cytoskeleton networks in the different conditions. As shown in Figure 4c,
261 while centrosomal actin decreases after CXCL12 stimulation, the level of polymerized microtubules

262 increases. Surprisingly, upon H89 addition, polymerized actin and microtubules both increase
263 suggesting a direct effect of PKA on microtubule polymerization/depolymerization equilibrium.
264
265 **Causal link between centrosomal F-Actin and cell deformation**
266 All the results presented above suggest a link between the level of centrosomal actin and cell shape.
267 We then attempted to investigate the potential causality between the two events. First, we
268 determined the temporality of the two events by following the two parameters in individual cells by
269 dynamic cell imaging. As shown in the example presented in Figure 4d, after chemokine stimulation,
270 the cell starts to deform (blue line) 70 seconds after centrosomal F-actin starts to decrease (black
271 line). The average value of the delay between these two events is 56 ± 12 seconds (n=26 individual
272 cells) showing that they are clearly sequential.
273 WASH is an actin nucleation-promoting factor which is able to activate Arp2/3 through its VCA
274 (Verprolin homology of WH2-connector-acidic) domain. Targeting this domain to the centrosome by
275 expressing the VCA-centrin1-GFP construct permits to artificially trigger an increase of F-Actin at this
276 place as previously reported (Obino et al, 2016). We therefore used this approach to analyze the
277 direct impact of centrosomal F-Actin on cell roundness. In CEM T cells, expression of the VCA-
278 centrin1 construct induces, as expected, a clear accumulation of F-Actin at the centrosome in non-
279 stimulated T lymphocytes as displayed on the examples (Fig Supp 8a) and quantified in Figure 4e
280 (left). Interestingly, the cells in which centrosomal F-Actin was artificially increased by VCA
281 expression, are less deformed as shown by a higher roundness value (Figure 4e right and examples in
282 Figure Supp 8b). Therefore, in resting cells, increasing the level of F-actin at the centrosome is
283 sufficient to trigger a rounding of the cells. In VCA-centrin1-GFP expressing cells, the CXCL12-
284 triggered signaling pathways leading to centrosomal actin reduction are still efficient. We then
285 observed that, unlike with PKA inhibitor, CXCL12 is able to decrease centrosomal actin as well as to
286 deform the cells. Of note, the values of both parameters measured in these conditions are not
287 significantly different from those measured in unstimulated control cells.

288 Altogether, our results show that 1) cell deformation appears after the decrease of centrosomal F-
289 Actin and 2) that any treatment, such as PKA inhibitors (H89 and Rp-8-CPT-cAMPS), AKAP inhibitor
290 Ht31 or centrin1-VCA, which lead to an increase in centrosomal F-Actin, also induces a rise in cell
291 roundness. Furthermore, although CXCL12 is still able, in these different conditions, to decrease
292 centrosomal F-actin, it does so moderately, so that centrosomal F-Actin always stays above the level
293 measured in control conditions and the cells remain less deformed than the resting cells. This
294 observation suggests that a decrease of centrosomal F-Actin at least below the resting value, has to
295 be reached for the cells to deform. In order to analyze this threshold, we measured concomitantly at
296 single cell level, centrosomal actin and cell roundness and determined after CXCL12 stimulation, the
297 value of actin at which the cell starts to deform. In the example presented in Figure 4d, the cell starts
298 to deform (blue line) when the centrosomal actin value is 0.8 (i.e. 20% decrease) (red arrow). By
299 analyzing a series of cells, we determined that centrosomal F-Actin has to be at 85 ± 2 % (n=26
300 individual cells) of the initial value for the cell to quit its resting shape.
301 The link between the level of actin at the centrosome and cell roundness we observed in our
302 experiments, can be visualized by the phase diagram-like graph presented in Figure 5a, where the
303 roundness has been plotted relative to the level of centrosomal actin. Each dot represents the mean
304 of many cells for which the two parameters have been measured. In each case, the values of
305 centrosomal F-actin and roundness have been normalized relative to the mean values measured in
306 unstimulated control cells of the same experiment (i.e no treatment for control, H89; Ht31-P for
307 Ht31; centrin1-GFP for VCA-centrin1-GFP). Therefore, control cells have (1,1) as coordinates. Four
308 quadrants can then be distinguished relative to the levels of normalized centrosomal actin or
309 normalized roundness. Clearly, the different values distribute into only two of the four quadrants
310 corresponding to round cells with a centrosomal F-Actin value >1 (orange area), or to deformed cells
311 with centrosomal F-Actin<1 (blue area). The two other configurations are not observed. This
312 observation suggests that centrosomal F-actin content behaves as a switch (when it reaches 85% of
313 the initial level) that toggles the cells from the round to the deformed state.

314 All the experiments presented above allows us to propose a sequential series of events leading to T
315 cell deformation: chemokine stimulation triggers a rapid rise in Ca, then in cAMP, followed by PKA
316 activation which triggers a decrease of polymerized actin around the centrosome. This step is a
317 prerequisite for deformation of the cell which precedes the opening of cortical actin cortex near the
318 centrosome to establish the polarity axis. This sequence is summarized in Figure 5b.
319

320 ## Discussion

321 T lymphocyte migration is an essential step to mount an efficient immune response (Krummel et al,
322 2016). It is essentially under the control of chemokines which trigger T cell polarization and
323 thereafter cell motility. These events require complete cellular reorganization in order for the cell to
324 acquire an asymmetrical distribution of its components (Mastrogiovanni et al, 2022). This then allows
325 the establishment of a lamellipodium and a uropod, which settle the polarization axis and therefore
326 the direction of migration (Pineau et al, 2023). Even in absence of chemokine gradient, cells polarize
327 in response to this external signal. In this study, we wondered, how the position of the polarity axis is
328 controlled in these conditions, and what are the signaling pathways involved. Our results obtained on
329 both CEM T cells and primary human T lymphocytes highlight a crucial role of the centrosome and
330 more precisely of a PKA-regulated pool of actin in the centrosomal zone.

331

332 ***PKA and response to chemokine***

333 Our results clearly identify the cAMP/PKA pathway as playing a key role in T cell response to
334 chemokine. In particular, we emphasize the involvement of a specific pool of PKA, anchored at the
335 centrosome through AKAP450. Consistent with our data, the deletion of the protein has been
336 previously reported to prevent T cell deformation and migration upon chemokine stimulation (Ong et
337 al, 2018).

338 The positive involvement of PKA in T cell polarization may be surprising for two reasons. First of all,
339 our results show, that CXCL12 stimulation is able to trigger a rapid rise in cAMP followed by PKA
340 activation, despite the fact that chemokine receptors are normally coupled to Gi proteins supposed
341 to inhibit adenylate cyclases. However, we show that, in our case the cAMP rise is mediated by the
342 chemokine-induced increase of calcium which precedes cAMP signal. This result may suggest the
343 involvement of an unidentified calcium-sensitive adenylate cyclase (such as AC1, AC3, AC8 or AC10
344 (Ostrom et al, 2022), (Steegborn, 2014), although AC7 has been reported to be the most abundant
345 adenylate cyclase in T cells (Duan et al, 2010). Secondly, cAMP/PKA have been considered as an

346 inhibitory pathway for T cell migration. This consideration is based on the fact that a large and
347 sustained increase in cAMP triggered by forskolin, PGE2 or phosphodiesterase inhibitors induces a
348 rounding up of the cells ((Valitutti et al, 1993), (Oppenheimer-Marks et al, 1994), (Layseca-Espinosa
349 et al, 2003), (Dong et al, 2006). However, after chemokine addition, the rise in cAMP remains modest
350 and transient. It is therefore likely that different features of cAMP signals (intensity and time course)
351 do not lead to the same effect as is the case for calcium, for which it is clearly established that the
352 shape of the signal conditions the cellular response (see (Berry et al, 2018) for a review).
353 Furthermore, with the combination of two properties of AKAP450, it is possible that this protein is
354 able to restrict the PKA signal at its close vicinity. First, it is able to bind different partners including
355 the phosphodiesterase PDE4D3 (Tasken et al, 2001), able to degrade cAMP, and then to reduce the
356 scale of the chemokine-induced cAMP increase. Secondly, the binding of PKA to AKAP450 reduces
357 the activation threshold of the kinase by cAMP (Terrin et al, 2012). This could allow a moderate
358 cAMP signal to trigger PKA activation only around the centrosome where AKAP450 is anchored, and
359 then to prevent the previously described inhibitory effect of this kinase.
360
361 ***Regulation of centrosomal actin in lymphocyte***
362 Recent studies in T and B lymphocytes demonstrate that, upon immune synapse formation, the pool
363 of actin around the centrosome is decreased (Obino et al, 2016), (Cassioli et al, 2021), (Ibanez-Vega
364 et al, 2019), (Bello-Gamboa et al, 2020). Here for the first time, we show that a similar process takes
365 place in response to chemokine. Using dynamic cell imaging and immunofluorescence, we were able
366 to show that this phenomenon takes place almost immediately after chemokine addition. In the case
367 of antigen recognition, the specific kinetics of this process has not been investigated, and the first
368 time point at which the decrease is reported is 15 minutes, but it is possible that the decrease starts
369 earlier. The level of actin at the centrosome results from a balance between the polymerization and
370 depolymerization processes at this site, so that a decrease of F-Actin after chemokine stimulation
371 might be due to an inhibition of the polymerization and/or activation of the depolymerization. In the

372 context of immune synapse, several non-exclusive mechanisms have been suggested to explain this
373 reduction in centrosomal actin (Cassioli & Baldari, 2022). Upon T/B synapse, the recruitment of HS1
374 at the synapse, triggers the displacement of Arp2/3 from the centrosome to the synapse and
375 therefore induces a reduction of F-Actin at this place (Obino et al, 2016). In our conditions, we
376 observed a similar reduction of Arp2/3 in the centrosomal area (Figure Supp 6), although we do not
377 know which mechanism drives it. The involvement of PKCδ and of the proteasome have also been
378 shown upon immune synapse formation (Cassioli et al, 2021), (Ibanez-Vega et al, 2019), (Bello-
379 Gamboa et al, 2020) but no evidence of the involvement of these pathways exists in the case of
380 chemokine stimulation. On the contrary, our results suggest that a local pool of PKA anchored to the
381 centrosome through an AKAP would control the level of F-actin at this place, not only after
382 chemokine stimulation, but also in resting cells. It is still unclear the mechanism by which PKA exerts
383 this effect and what is the target(s) it phosphorylates.
384 In resting cells, the centrosome presents an eccentric positioning which corresponds to its minimum-
385 energy position (Maly, 2011) and is controlled by actin-myosin network (Jimenez et al, 2021).
386 However, during cellular responses, its position seems to be finely regulated (Kroll & Renkawitz,
387 2024), especially in T lymphocytes during chemokine-triggered polarization or immune synapse
388 formation, where a relocation of the centrosome is observed. Centrosomal actin seems to contribute
389 to the stabilization of the centrosome (Yamamoto et al, 2022) and, in B lymphocytes, to its anchoring
390 to the nucleus through the LINC complex (Obino et al, 2016). One could then imagine that the
391 decrease of centrosomal actin after chemokine stimulation which we observe in our study, allows the
392 reduction of centrosome anchoring to the nucleus, a necessary step for the relocation of the
393 centrosome behind the nucleus during migration. The front position of the nucleus constitutes
394 indeed a specific characteristic of amoeboid migration permitting the cell to gauge the environment
395 and to perform optimal migration (Kroll et al, 2023), (Renkawitz et al, 2019). Corroborating this
396 hypothesis, with a siRNA screen, Obino *et al* recently identified, which proteins among those
397 differentially associated to the centrosome upon B cells stimulation, are important for centrosome

398 movement. Type II regulatory subunit beta and catalytic subunit beta of PKA appear in this list (Obino
399 et al, 2023).
400 Our study highlights a central role of PKA-regulated centrosomal actin upon uniform chemokine
401 stimulation. However, one can wonder what would happen in the case of chemokine gradient, as
402 frequently observed *in vivo*. Would the cells polarize along the gradient independently of the
403 centrosome position? Would the centrosome, whatever its position relatively to the gradient, impose
404 the polarization axis? Or, finally as a mix of the two previous possibilities, would the cell rotate in
405 order to position the centrosome according to the gradient?
406
407 ***Centrosomal actin, cell deformation and lamellipodium formation***
408 Besides the potential role of centrosomal actin in controlling the centrosome mobility, our results
409 suggest that it also regulates the shape of the cells in resting conditions, as well as after chemokine
410 stimulation. What is the link between these two events? Several non-exclusive hypotheses can be
411 suggested. Firstly, it has been shown recently that actin (rather than microtubules) around the
412 centrosome can be a cage that limits the exchange between the cytoplasm and the pericentriolar
413 region (Cheng et al, 2022). A decrease of actin in this area would then weaken this barrier and
414 potentially lead to modification of the centrosomal composition. Interestingly, that is what is
415 observed by Obino *et al*, who showed, in parallel to immune synapse formation, a decrease in
416 centrosomal actin as well as a modification of the protein content associated with the centrosome:
417 some leave this area, while some are recruited (Obino et al, 2016). A similar process could probably
418 take place in our case, after stimulation by chemokine. Because some of these proteins belong to
419 signaling pathways, this local actin modification will influence local signaling events which may be
420 important for centrosome relocation and for the cellular response. Among these proteins, as
421 mentioned above, Arp2/3 leaves the centrosome upon immune synapse formation, as well as after
422 chemokine stimulation (Figure Supp 6). This major actin branching protein can be considered as a
423 fundamental brick for actin network formation at the lamellipodium, so that triggering its release is

424 crucial. On the other hand, the disappearance of the actin cage around the centrosome seems to also
425 allow the recruitment of new proteins at this site. This is particularly the case of Dock2, an exchange
426 factor of the small GTPase Rac, a crucial element for actin polymerization in T cells. It is then possible
427 that the local activation of Rac through Dock2 triggers actin polymerization, and the subsequent
428 formation of the lamellipodium in this area. Finally, the decrease of the centrosomal actin pool can
429 have some consequences on microtubules network which controls cell shape and contributes to cell
430 directionality although it is dispensable for T cell migration (Kopf & Kiermaier, 2021). Indeed, actin
431 and microtubule networks at the centrosome have been reported to be dynamically connected so
432 that actin level tunes microtubules and vice-versa (Inoue et al, 2019). This might result from the fact
433 that centrosomal F-Actin could constitute a physical barrier preventing microtubule elongation
434 (Cheng et al, 2022). The local decrease of centrosomal actin could therefore be essential for the
435 extension of the microtubule network and the subsequent centrosome repositioning (Yamamoto et
436 al, 2022). In line with these results, we have observed in our model that CXCL12-induced decrease of
437 F-actin at the centrosome is accompanied by an increase of microtubules in this area and can then be
438 essential for T cell polarization. However, in an unexpected way, the PKA inhibitor H89 triggers
439 increases of both polymerized actin and microtubules. This suggests that, besides the supposed
440 balance between the two cytoskeleton networks, PKA might directly promote microtubule
441 depolymerization (or inhibit their polymerization) for instance through Microtubule-Associated
442 Proteins whose activity can be affected by phosphorylation (Ramkumar et al, 2017).
443 Our results highlight that a 15 ± 2% reduction of centrosomal actin switches the cells from a round
444 state to a deformed one (summary in Figure 5a). The biological meaning of this threshold is unclear,
445 but it could correspond to the reduction of the size of the actin mesh. Indeed, Cheng *et al* highlight
446 that centrosomal actin behave as a protein sieve, and that the reduction of its amount allows the
447 centrosome accessibility of proteins with a higher Stockes radius (Cheng et al, 2022). One could then
448 imagine that a 15% reduction of centrosomal actin is the necessary decrease for recruiting (or

449 loosing) the specific proteins, mentioned above, which are necessary for the T cell morphological
450 change.
451 Altogether our results highlight a central role of PKA in the establishment of the polarization axis
452 upon chemokine stimulation. These results establish a new example where transient activation of
453 PKA promote an efficient T cell response (Simao et al, 2021) (Conche et al, 2009), contrary to large
454 and sustained activation which trigger some immunoinhibitory effects (Postler, 2021).
455
456

457 # Materials & Methods

458 **Cell culture and PBT purification**

459 CEM, a human T lymphoblast cell line isolated from a patient with lymphoblastic leukemia, were
460 cultured in RPMI 1640 GlutaMax (Gibco, #61870010), supplemented with 10% FCS, 50 U/ml penicillin
461 and 50 µg/ml streptomycin (Eurobio CABPES01-OU). When specified, cells were transfected by
462 nucleofection (Amaxa Nucleofactor, Lonza VCA-1003) with 5 µg DNA for 5 million of cells using the C-
463 016 program. The cells were used the day after nucleofection.

464 Peripheral blood samples from healthy adult individuals were obtained from EFS (Etablissement
465 Français du Sang) under agreement 18/EFS/030, including informed consent for research purposes.
466 Blood samples were anonymous and not associated with any personal data (including age, gender, or
467 sex). Human peripheral blood mononuclear cells (PBMCs) were isolated using Ficoll gradient (800g
468 for 20min, RT) and T cells were purified using Pan T cell Isolation Kit (Miltenyi, 130-096-535). Human
469 T cells cultured in RPMI 1640 GlutaMax supplemented with 10% Human AB serum (Biowest, #S4190–
470 100), 50 U/ml penicillin and 50 µg/ml streptomycin (Eurobio CABPES01-OU) were used for
471 experiments the day after purification.

472

473 **Reagents**

474 CXCL12 (recombinant human SDF1-α) was purchased from Peprotech (300-28A) and VCAM-1 (CD106
475 Fc chimera protein) from R&D Systems (862-VC-100). Calcium measurements were performed with
476 Fura-2/AM (Molecular Probes, F1225). For calcium chelation, cells were incubated with 20µM
477 BAPTA-AM (ThermoFisher B6769) for 30 minutes. Nucleus labeling was performed for 4 minutes with
478 2µg/ml Hoechst 33342 (Molecular Probes, H1399). F-actin detection was performed by expressing
479 the LifeAct-mCherry construct (gift from Dr. A. Benmerah) or with AlexaFluor488 or AlexaFluor568
480 conjugated phalloidin (Life Technologies, A12379 or A12380, 1/1000). Stable actin detection was
481 performed with SiRActin (TebuBio, SC001) as previously described (Siamo et al, 2021). Centrin1-GFP
482 was a gift from Dr. A. Delouvée (Institut Curie, Paris, France) and Centrin1-VCA-GFP and Centrin1-GFP

483 were obtained from Dr. Paolo Pierobon (Institut Cochin, Paris). For cAMP measurements, cells were
484 transfected with the most sensitive version of TEpacVV (H187), which was a gift from Dr. K. Jalink
485 (Netherlands Cancer Institute). Monitoring of PKA activity is achieved through the expression of the
486 ExRaiAKAR2 construct (Addgene, #161753). For PKA activity inhibition, cells were pretreated with
487 10µM of H89 (Calbiochem, 371963), 200 µM Rp-8CPT-cAMPS (Biolog, B001 & C011) for 30 minutes.
488 For PKA delocalization from type II AKAPs, cells were pretreated with 20µM of the inhibitory peptide
489 Ht31 (RRRRRRRRRLIEEAASRIVDAVIEQV) or the control peptide Ht31-P
490 (RRRRRRRRRLIPEAASRPVDAVIEQV) for 1 hour (synthetized by ProteoGenix).
491 The following primary antibodies were used for immunofluorescence: mouse anti-pericentrin
492 (Abcam, #28144, 1/1000), rabbit anti-pericentrin (Abcam, #4448, 1/2000), rabbit anti-Arp2 (Abcam,
493 #47654, 1/200), anti-AKAP450 (Becton Dickinson 611518, 1/50), Mouse anti CXCR4 human (R et D
494 Systems, #MAB172, 1/200), Mouse anti-α tubulin (Sigma T9026, 1/1000), Mouse anti PKA Cα (Becton
495 Dickinson 610981, 1/50). Secondary antibodies were the following: AlexaFluor568 donkey anti-
496 mouse, AlexaFluor647 donkey anti-rabbit and AlexaFluor plus 647 donkey anti-mouse (Life
497 Technologies, A10037, A32787 and A31573, 1/1000 or 1/500).
498
499 **Cell stimulation and labelling**
500 For cell roundness measurements, cells were deposited on coverslips coated with 1µg/ml VCAM-1
501 and, when specified, 1µg/ml CXCL12 (except for Figure 2g, 0.3µg/ml) and kept at 37°C for the
502 indicated time. This type of stimulation allows the cells to polarize in the plane of the coverslip and
503 thus to quantify the deformation. For immunofluorescence experiments, cells were deposited on
504 coverslips coated with 1µg/ml VCAM-1 and, after 5 minutes adhesion, 100ng/ml CXCL12 (except for
505 Figure 3d, 25ng/ml) was added to the medium, allowing synchronized stimulation and therefore
506 more precise measurements of the kinetics.
507 Cells were fixed with 4% paraformaldehyde for 20 minutes at room temperature. Cells were then
508 permeabilized for 20 minutes with PBS-BSA-Saponin (1x / 0.5% / 0.1%), incubated for 45 minutes

509 with the primary antibody and 45 minutes more with the secondary antibody and fluorescent
510 phalloidin. For CXCR4, the labelling was performed on unpermeabilized cells.
511 For Tubulin and PKA staining, cells were fixed with 4% PFA + 0.2% Glutaraldehyde in PHEM solution
512 (60 mM PIPES, 25 mM HEPES, 10mM EGTA, 2mM Mg acetate) + 0.5% Triton, for 12 minutes. Cells
513 were then permeabilized for 20 minutes with PBS-BSA-Saponin (1x / 0.5% / 0.1%), incubated for 45
514 minutes with the primary antibody and 45 minutes more with the secondary antibody and
515 fluorescent phalloidin.
516 Coverslips were mounted with Fluorsave (Millipore, #345789). Microscopy images were acquired
517 with a wide field microscope, Nikon Eclipse TE2000-U and a CMOS camera CMOS camera (ORCA-
518 flash4.0 LT, Hamamatsu). Images were acquired with Metamorph software with a 20x/0.75 objective
519 (morphology measurements) or 60x or 100x/0.5-1.3 oil immersion objective (fluorescence
520 quantification).
521
522 **Time-lapse imaging and analysis**
523 Live imaging experiments were performed at 37°C with a wide-field Nikon TE2000, equipped with a
524 CMOS camera (ORCA-flash4.0 LT, Hamamatsu). Images were acquired every 10 s with Metafluor
525 software. For monitoring Ca, cAMP, PKA activity and centrosomal actin, a 40x/1.30 oil immersion
526 objective was used. The dynamic imaging experiments are all performed in saline medium (140 mM
527 NaCl, 5 mM KCl, 1mM CaCl2, 1mM MgCl2, 11mM glucose, 10 mM Hepes; pH 7.4).
528 In all figures and for each individual cell, traces have been normalized to the ratio at the time of the
529 stimulation (R/R0) before averaging.
530 *cAMP*
531 cAMP measurements were performed with the FRET biosensor TEpacVV. Briefly, when cAMP
532 increases, the probe undergoes a conformational change that allows a decrease of energy transfer
533 between the turquoise fluorophore and the two Venus molecules. Three images were acquired every
534 10 s: visible, Turquoise channel and FRET channel. The ratio $R = I_{436/470}/I_{436/535}$, which gives an

535 estimate of cAMP concentration, was calculated with MetaFluor (Roper Scientific) after background
536 subtraction. An increase of this ratio corresponds to an increase in cAMP concentration.

537 *PKA activity*

538 cAMP measurements were performed with PKA biosensor ExRaiAKAR2 possessing a circularly
539 permuted GFP (cpGFP). Upon PKA phosphorylation of the probe, a conformation change shifts the
540 maximum excitation wavelength from 400 nm to 480 nm. Three images were acquired every 10s:
541 visible, Exc 480nm / Em 515nm and Exc 405nm /Em 515nm. The ratio $R = I_{480/515}/I_{405/515}$ is
542 calculated with MetaFluor after subtraction of the background noise. An increase of this ratio
543 corresponds to an increase in PKA activity.

544 *Simultaneous Ca and cAMP measurements*

545 Cells transfected with TEpacVV were loaded with Fura-2/AM at a low concentration (50nM) in order
546 to avoid interferences between the different fluorophores. 5 images were acquired every 10s: visible,
547 Exc 340nm / Em 510 nm, Exc 380 nm / Em 510 nm, Exc 436 nm/ Em 470 nm, Exc 436 nm, Em 535 nm.
548 The ratios $R = I_{340/510}/I_{380/510}$ and $R = I_{436/470}/I_{436/535}$, which give an estimate of Ca and cAMP
549 concentrations respectively, were calculated with MetaFluor (Roper Scientific) after background
550 subtraction.

551

552 **Image analysis**

553 *Cell roundness*

554 Cell roundness parameter was quantified with ImageJ software and corresponds to:
555 $4 \times \mathrm{area}/\pi \times (\mathrm{major\ axis})^2$. It is equal to 1 for a round cell and < 1 for a deformed one.

556 *Centrosome position quantification*

557 CEM cells transfected with centrin1-GFP and labeled with SiRActin were deposited on a VCAM-1-
558 coated coverslip for 5 minutes before adding CXCL12. The images were acquired every 10 seconds.
559 The image corresponding to the opening of the actin cortex was determined by watching movies and
560 considered only relatively to previous and the next ones. Indeed, we first determined the period

561 when 1/ SiRActin labeling stably decreases at one pole of the cell and 2/ the cell simultaneously
562 deforms (transmitted light pictures). Playing the sequence backward, allowed us to determine the
563 beginning of cortex opening. At this time, we collected the coordinates of the centrosome, the cell
564 center and the actin cortex opening. Based on this information, we calculated the angle between the
565 two lines [Center of the cell - Center of the opening of cortical actin cage] and [Center of the cell -
566 Centrosome].

567 *Centrosomal actin and Arp2 quantification*

568 Accumulation of Actin or Arp2 around the centrosome is quantified by measuring integrated
569 intensities of the labelling in a circle of 1.5µm radius, centred on the centrosome (pericentrin or
570 centrin labelling). A background value is subtracted from this measurement, corresponding to the
571 integrated intensity measured in a similar circle, designed in the cell but outside of the centrosome
572 area.

573 *Quantification of centrosomal PKA Cα accumulation*

574 Accumulation of PKA Cα at the centrosome is quantified by calculating the ratio between integrated
575 intensities of the labelling in a circle of 1.5µm radius, centred on the centrosome with the one
576 measured in a circle of 1.5µm radius positioned in the cytoplasm. A ratio superior to 1 means that
577 the protein is enriched around the centrosome.

578 *Pearson coefficient*

579 Pearson coefficient was measured on ImageJ by using a macro containing the Coloc2 plugin. This
580 coefficient measures the degree of overlap between two stainings: perincentrin and AKAP450. A
581 Pearson Coefficient value of 0 means that there is no colocalization between the two stainings.
582 Conversely, a Pearson Coefficient value of 1 means that there is a perfect colocalization.

583

584 **Migration assay**

585 The migration assay was performed as previously described (Megrelis & Delon, 2014). Briefly, 300µl
586 of CEM cells (1M/ml, complete medium) were deposited in the upper compartment of a Transwell

587 insert (pore diameter: 5µm; Nunc). When indicated, the cells were pre-incubated with 10µM H89 for
588 30min. The lower compartment contained no chemokine or 200 ng/ml CXCL12 in 600µl of complete
589 medium. In H89 conditions, the drug was also added to the two compartments during the migration
590 assay. After 2 h of incubation, the inserts were removed, an equal amount of 10 µl calibration beads
591 (Flow-Check Fluorospheres, Beckman Coulter) was deposited in the wells, and the number of cells
592 having migrated to the lower compartment relative to the number of beads was quantified by flow
593 cytometry (FACS Calibur, BD). In parallel, 300µl of CEM cells (1M/ml, complete medium) were
594 incubated for 2h in wells without insert containing 600µl of complete medium. 10µM H89 were
595 added when indicated. The total amount of cells in these wells was then measured through the same
596 method. Migration was quantified in each condition as the number of migrating cells/total cell
597 number x 100.
598
599 **Statistics**
600 Each experiment was repeated N times, as specified in the figure legends, along with the number of
601 cells analyzed in each experiment for a given condition. Data were formatted with Prism Software. In
602 the paper, mean ± SE are indicated. Statistical comparisons were performed with Jamovi software
603 through t-test (Figure 2c), paired t-test (Figure Supp 7b) or non-parametric Anova test for multiple
604 comparisons (Friedman for paired experiments or Kruskal-Wallis for unpaired ones). 2way Anova was
605 used for curve comparisons. * $p<0.05$, ** $p<0.01$, *** $p<0.001$, **** $p<0.0001$.
606
607 **Acknowledgements**
608 We thank Luca Simula for human primary T cells purification, G. Pidoux for helpful discussions on
609 AKAP, J. Delon and P. Pierobon for helpful discussions and comments on the manuscript.
610
611 **Funding**
612 This work was supported by CNRS, Inserm and Université Paris Cité. M.S. was supported by the
613 Ministère de l'Enseignement Supérieur et de la Recherche and by the Labex Who Am I?.

614

615 **Author contributions**

616 M.S., F.R. and C.R. designed and performed experiments and analyzed data. M.S. and C.R. wrote the

617 manuscript.

618 **Competing interests**

619 The authors declare no competing interests

620

621 **References**
622
623 Arige V, Yule DI (2022) Spatial and temporal crosstalk between the cAMP and Ca(2+) signaling
624 systems. *Biochim Biophys Acta Mol Cell Res* **1869**(9)**:** 119293
625
626 Bello-Gamboa A, Velasco M, Moreno S, Herranz G, Ilie R, Huetos S, Davila S, Sanchez A, Bernardino
627 De La Serna J, Calvo V, Izquierdo M (2020) Actin reorganization at the centrosomal area and the
628 immune synapse regulates polarized secretory traffic of multivesicular bodies in T lymphocytes. *J*
629 *Extracell Vesicles* **9**(1)**:** 1759926
630
631 Berry CT, May MJ, Freedman BD (2018) STIM- and Orai-mediated calcium entry controls NF-kappaB
632 activity and function in lymphocytes. *Cell Calcium* **74:** 131-143
633
634 Cassioli C, Baldari CT (2022) Lymphocyte Polarization During Immune Synapse Assembly:
635 Centrosomal Actin Joins the Game. *Front Immunol* **13:** 830835
636
637 Cassioli C, Onnis A, Finetti F, Capitani N, Brunetti J, Compeer EB, Niederlova V, Stepanek O, Dustin
638 ML, Baldari CT (2021) The Bardet-Biedl syndrome complex component BBS1 controls T cell polarity
639 during immune synapse assembly. *J Cell Sci* **134**(16)
640
641 Cheng H, Kao YL, Chen T, Sharma L, Yang WT, Chuang YC, Huang SH, Lin HR, Huang YS, Kao CL, Yang
642 LW, Bearon R, Cheng HC, Hsia KC, Lin YC (2022) Actin filaments form a size-dependent diffusion
643 barrier around centrosomes. *EMBO Rep***:** e54935
644
645 Conche C, Boulla G, Trautmann A, Randriamampita C (2009) T cell adhesion primes antigen receptor-
646 induced calcium responses through a transient rise in adenosine 3',5'-cyclic monophosphate.
647 *Immunity* **30**(1)**:** 33-43
648
649 Davies SP, Reddy H, Caivano M, Cohen P (2000) Specificity and mechanism of action of some
650 commonly used protein kinase inhibitors. *Biochem J* **351**(Pt 1)**:** 95-105
651
652 Dong H, Osmanova V, Epstein PM, Brocke S (2006) Phosphodiesterase 8 (PDE8) regulates chemotaxis
653 of activated lymphocytes. *Biochem Biophys Res Commun* **345**(2)**:** 713-719
654
655 Duan B, Davis R, Sadat EL, Collins J, Sternweis PC, Yuan D, Jiang LI (2010) Distinct roles of adenylyl
656 cyclase VII in regulating the immune responses in mice. *J Immunol* **185**(1)**:** 335-344
657
658 El Din El Homasany BS, Volkov Y, Takahashi M, Ono Y, Keryer G, Delouvee A, Looby E, Long A,
659 Kelleher D (2005) The scaffolding protein CG-NAP/AKAP450 is a critical integrating component of the
660 LFA-1-induced signaling complex in migratory T cells. *J Immunol* **175**(12)**:** 7811-7818
661
662 Elric J, Etienne-Manneville S (2014) Centrosome positioning in polarized cells: common themes and
663 variations. *Exp Cell Res* **328**(2)**:** 240-248
664
665 Farina F, Gaillard J, Guerin C, Coute Y, Sillibourne J, Blanchoin L, Thery M (2015) The centrosome is an
666 actin-organizing centre. *Nat Cell Biol* **18**(1)**:** 65-75
667
668 Gjertsen BT, Mellgren G, Otten A, Maronde E, Genieser HG, Jastorff B, Vintermyr OK, McKnight GS,
669 Doskeland SO (1995) Novel (Rp)-cAMPS analogs as tools for inhibition of cAMP-kinase in cell culture.
670 Basal cAMP-kinase activity modulates interleukin-1 beta action. *J Biol Chem* **270**(35)**:** 20599-20607
671

672 Ibanez-Vega J, Del Valle Batalla F, Saez JJ, Soza A, Yuseff MI (2019) Proteasome Dependent Actin
673 Remodeling Facilitates Antigen Extraction at the Immune Synapse of B Cells. *Front Immunol* **10:** 225
674
675 Inoue D, Obino D, Pineau J, Farina F, Gaillard J, Guerin C, Blanchoin L, Lennon-Dumenil AM, Thery M
676 (2019) Actin filaments regulate microtubule growth at the centrosome. *EMBO J* **38**(11)
677
678 Jimenez AJ, Schaeffer A, De Pascalis C, Letort G, Vianay B, Bornens M, Piel M, Blanchoin L, Thery M
679 (2021) Acto-myosin network geometry defines centrosome position. *Curr Biol* **31**(6)**:** 1206-1220
680 e1205
681
682 Kameritsch P, Renkawitz J (2020) Principles of Leukocyte Migration Strategies. *Trends Cell Biol* **30**(10)**:**
683 818-832
684
685 Kehrl JH (2006) Chemoattractant receptor signaling and the control of lymphocyte migration.
686 *Immunol Res* **34**(3)**:** 211-227
687
688 Klarenbeek J, Goedhart J, van Batenburg A, Groenewald D, Jalink K (2015) Fourth-generation epac-
689 based FRET sensors for cAMP feature exceptional brightness, photostability and dynamic range:
690 characterization of dedicated sensors for FLIM, for ratiometry and with high affinity. *PLoS One* **10**(4)**:**
691 e0122513
692
693 Kloc M, Kubiak JZ, Li XC, Ghobrial RM (2014) The newly found functions of MTOC in immunological
694 response. *J Leukoc Biol* **95**(3)**:** 417-430
695
696 Kopf A, Kiermaier E (2021) Dynamic Microtubule Arrays in Leukocytes and Their Role in Cell
697 Migration and Immune Synapse Formation. *Front Cell Dev Biol* **9:** 635511
698
699 Kroll J, Hauschild R, Kuznetcov A, Stefanowski K, Hermann MD, Merrin J, Shafeek L, Muller-
700 Taubenberger A, Renkawitz J (2023) Adaptive pathfinding by nucleokinesis during amoeboid
701 migration. *EMBO J* **42**(24)**:** e114557
702
703 Kroll J, Renkawitz J (2024) Principles of organelle positioning in motile and non-motile cells. *EMBO*
704 *Rep* **25**(5)**:** 2172-2187
705
706 Krummel MF, Bartumeus F, Gerard A (2016) T cell migration, search strategies and mechanisms. *Nat*
707 *Rev Immunol* **16**(3)**:** 193-201
708
709 Langlois-Lemay L, D'Amours D (2022) Moonlighting at the Poles: Non-Canonical Functions of
710 Centrosomes. *Front Cell Dev Biol* **10:** 930355
711
712 Layseca-Espinosa E, Baranda L, Alvarado-Sanchez B, Portales-Perez D, Portillo-Salazar H, Gonzalez-
713 Amaro R (2003) Rolipram inhibits polarization and migration of human T lymphocytes. *J Invest*
714 *Dermatol* **121**(1)**:** 81-87
715
716 Maly IV (2011) Systems biomechanics of centrosome positioning: A conserved complexity. *Commun*
717 *Integr Biol* **4**(2)**:** 230-235
718
719 Mastrogiovanni M, Di Bartolo V, Alcover A (2022) Cell polarity regulators, multifunctional organizers
720 of lymphocyte activation and function. *Biomed J* **45**(2)**:** 299-309
721
722 Megrelis L, Delon J (2014) Rapid and robust analysis of cellular and molecular polarization induced by
723 chemokine signaling. *J Vis Exp*(94)

724
725 Murray AJ (2008) Pharmacological PKA inhibition: all may not be what it seems. *Sci Signal* **1**(22)**:** re4
726
727 Niggli V (2014) Insights into the mechanism for dictating polarity in migrating T-cells. *Int Rev Cell Mol*
728 *Biol* **312:** 201-270
729
730 Obino D, Farina F, Malbec O, Saez PJ, Maurin M, Gaillard J, Dingli F, Loew D, Gautreau A, Yuseff MI,
731 Blanchoin L, Thery M, Lennon-Dumenil AM (2016) Actin nucleation at the centrosome controls
732 lymphocyte polarity. *Nat Commun* **7:** 10969
733
734 Obino D, Maurin M, Dingli F, Loew D, Lescure A, Terriac E, Goudot C, Malbec O, Lankar D, Yuseff MI,
735 Lennon-Dumenil AM, Moreau HD (2023) Medium-throughput image-based phenotypic siRNA screen
736 to unveil the molecular basis of B cell polarization. *Sci Data* **10**(1)**:** 401
737
738 Ong ST, Chalasani MLS, Fazil M, Prasannan P, Kizhakeyil A, Wright GD, Kelleher D, Verma NK (2018)
739 Centrosome- and Golgi-Localized Protein Kinase N-Associated Protein Serves As a Docking Platform
740 for Protein Kinase A Signaling and Microtubule Nucleation in Migrating T-Cells. *Front Immunol* **9:** 397
741
742 Oppenheimer-Marks N, Kavanaugh AF, Lipsky PE (1994) Inhibition of the transendothelial migration
743 of human T lymphocytes by prostaglandin E2. *J Immunol* **152**(12)**:** 5703-5713
744
745 Ostrom KF, LaVigne JE, Brust TF, Seifert R, Dessauer CW, Watts VJ, Ostrom RS (2022) Physiological
746 roles of mammalian transmembrane adenylyl cyclase isoforms. *Physiol Rev* **102**(2)**:** 815-857
747
748 Pineau J, Moreau H, Dumenil AL, Pierobon P (2023) Polarity in immune cells. *Curr Top Dev Biol* **154:**
749 197-222
750
751 Postler TS (2021) A most versatile kinase: The catalytic subunit of PKA in T-cell biology. *Int Rev Cell*
752 *Mol Biol* **361:** 301-318
753
754 Ramkumar A, Jong BY, Ori-McKenney KM (2017) ReMAPping the microtubule landscape: How
755 phosphorylation dictates the activities of microtubule-associated proteins. *Dev Dyn* **247**(1)**:** 138-155
756
757 Real E, Faure S, Donnadieu E, Delon J (2007) Cutting edge: Atypical PKCs regulate T lymphocyte
758 polarity and scanning behavior. *J Immunol* **179**(9)**:** 5649-5652
759
760 Renkawitz J, Kopf A, Stopp J, de Vries I, Driscoll MK, Merrin J, Hauschild R, Welf ES, Danuser G, Fiolka
761 R, Sixt M (2019) Nuclear positioning facilitates amoeboid migration along the path of least resistance.
762 *Nature* **568**(7753)**:** 546-550
763
764 Schatten H (2008) The mammalian centrosome and its functional significance. *Histochem Cell Biol*
765 **129**(6)**:** 667-686
766
767 Shellard A, Mayor R (2020) All Roads Lead to Directional Cell Migration. *Trends Cell Biol* **30**(11)**:** 852-
768 868
769
770 Simao M, Regnier F, Taheraly S, Fraisse A, Tacine R, Fraudeau M, Benabid A, Feuillet V, Lambert M,
771 Delon J, Randriamampita C (2021) cAMP Bursts Control T Cell Directionality by Actomyosin
772 Cytoskeleton Remodeling. *Front Cell Dev Biol* **9:** 633099
773
774 Steegborn C (2014) Structure, mechanism, and regulation of soluble adenylyl cyclases - similarities
775 and differences to transmembrane adenylyl cyclases. *Biochim Biophys Acta* **1842**(12 Pt B)**:** 2535-2547

Tasken KA, Collas P, Kemmner WA, Witczak O, Conti M, Tasken K (2001) Phosphodiesterase 4D and protein kinase a type II constitute a signaling unit in the centrosomal area. *J Biol Chem* **276**(25)**:** 21999-22002

Terrin A, Monterisi S, Stangherlin A, Zoccarato A, Koschinski A, Surdo NC, Mongillo M, Sawa A, Jordanides NE, Mountford JC, Zaccolo M (2012) PKA and PDE4D3 anchoring to AKAP9 provides distinct regulation of cAMP signals at the centrosome. *J Cell Biol* **198**(4)**:** 607-621

Thelen M, Stein JV (2008) How chemokines invite leukocytes to dance. *Nat Immunol* **9**(9)**:** 953-959

Valitutti S, Dessing M, Lanzavecchia A (1993) Role of cAMP in regulating cytotoxic T lymphocyte adhesion and motility. *EurJImmunol* **23:** 790-795

Yamamoto S, Gaillard J, Vianay B, Guerin C, Orhant-Prioux M, Blanchoin L, Thery M (2022) Actin network architecture can ensure robust centering or sensitive decentering of the centrosome. *EMBO J* **41**(20)**:** e111631

Zhang JF, Liu B, Hong I, Mo A, Roth RH, Tenner B, Lin W, Zhang JZ, Molina RS, Drobizhev M, Hughes TE, Tian L, Huganir RL, Mehta S, Zhang J (2020) An ultrasensitive biosensor for high-resolution kinase activity imaging in awake mice. *Nat Chem Biol* **17**(1)**:** 39-46

798 ## Figure Legends

799 **Figure 1: Chemokine stimulation triggers actin remodeling along an axis conditioned by MTOC**
800 **position**

801 a- Cell roundness progressively decreases in CEM T cells deposited for different periods of time, on
802 coverslips coated with VCAM-1 + CXCL12. A limited deformation takes place with VCAM-1 alone.
803 Mean ± SE of 4 independent experiments, 448-1722 cells/condition/experiment.

804 b- Acute addition of CXCL12 triggers rapid cell deformation (Mean ± SE of 48 individual cells).

805 c- Example of actin cortex opening after CXCL12 stimulation (red arrow) in a CEM T cell transfected
806 with Centrin1-GFP (red) and whose actin cortex has been labelled with SiRActin (green). Scale bar =
807 10µm.

808 d- As depicted in the scheme (top left), the angle formed by the two lines [Center of the cell (CC) -
809 Center of the opening of cortical actin cage (CO)] and [Center of the cell – Centrosome (CT)] has been
810 quantified in 60 cells. The distribution of the angles measured in similar experimental conditions as
811 (c) is shown in the rose (up right) and pie plots (bottom).

812

813 **Figure 2: Chemokine stimulation triggers a rapid increase in cAMP and activation of PKA necessary**
814 **for cell deformation**

815 a- CXCL12 addition triggers a rapid rise in cAMP in CEM T cells transfected with TEpacVV biosensor.
816 Mean ± SE of 6 independent experiments, 6-59 cells/experiment.

817 b- CXCL12 addition triggers a rapid rise in PKA activity in CEM T cells transfected with ExRaiAKAR2
818 biosensor. Mean ± SE of 6 independent experiments, 11-46 cells/experiment.

819 c- Quantification of the delay between CXCL12 addition and cAMP or PKA activity increases (first
820 point above the baseline). Mean ± SE of 139 cells (cAMP) and 201 cells (PKA).

821 d- Examples of CEM T cells transfected with TEpacVV (left) or ExRaiAKAR2 (right) and stimulated with
822 CXCL12. cAMP (left) or PKA activity (right) are low in resting cells, but rapidly increase after CXCL12

823 addition (red arrow). Cell deformation starts thereafter. cAMP and PKA activity are coded in false
824 color. Time 0: CXCL12 addition. Scale bar = 10µm.
825 e- Example of a simultaneous measurement of PKA activity (black line) and cell roundness (blue line)
826 in a CEM T cell transfected with exRaiAKAR2. The delay between the increase of PKA activity and the
827 beginning of cell roundness decrease is indicated by the gray arrow.
828 f & g- Pretreatment with H89 (f) or Rp-8CPT-cAMPS (g) of CEM T cells deposited on VCAM-1 or
829 VCAM1+CXCL12 coated-coverslips for 5 minutes, induces an increase of basal cell roundness and a
830 reduction of the chemokine-induced cell deformation. CXCL12 1µg/ml in (f) and 0.3µg/ml (g). Mean ±
831 SE of 6 independent experiments, 264-1475 cells/condition/experiment (f). Mean ± SE of 6
832 independent experiments, 479-1283 cells/condition/experiment (g).
833
834 **Figure 3: Chemokine stimulation triggers PKA-induced decrease of polymerized actin at the**
835 **centrosome**
836 a- Polymerized actin around the centrosome measured in a 3µm diameter area (inset) decreases
837 progressively in CEM T cells deposited on VCAM-1 or VCAM-1+CXCL12 for the indicated duration. For
838 each experiment, values have been normalized relatively to the mean intensity of centrosomal F-
839 actin measured in unstimulated cells. Mean ± SE of 8-10 independent experiments, 21-159
840 cells/condition/experiment.
841 b- Examples of F-Actin (labelled with phalloidin) distribution around the centrosome (detected by
842 anti-pericentrin antibodies) in untreated cells (control), stimulated with CXCL12 or simply pretreated
843 with H89. Scale bar = 10µm. Zooms of the indicated regions are shown below.
844 c & d- CEM T cells preincubated with H89 (c) or Rp-8CPT-cAMPS (d) display a higher level of
845 centrosomal actin in resting conditions compared to non-stimulated cells. After 5 minute stimulation
846 with CXCL12 (100 ng/ml (c) or 25 ng/ml (d)), this content is reduced but still remains above that of
847 resting cells (dotted line). For each experiment, values have been normalized relatively to the mean
848 intensity of centrosomal F-actin measured in untreated and unstimulated cells. Mean ± SE of 5

849 independent experiments, 22-165 cells/condition/experiment (c). Mean ± SE of 4 independent
850 experiments, 36-94 cells/condition/experiment (d).
851 e- Dynamic evolution of centrosomal actin in CEM T cells transfected with LifeAct-mCherry and
852 centrin1-GFP after addition (arrow) of DMSO (black trace), CXCL12 (red trace) or H89 (blue trace). For
853 each cell, intensity values have been normalized relatively to the value at the time of stimulation.
854 Mean ± SE of 19-30 cells/condition.
855 Lower panel: Example of centrosomal actin evolution after CXCL12 addition (red arrow) to CEM T
856 cells transfected with LifeAct-mCherry and centrin1-GFP. Scale bar = 10µm.
857
858 **Figure 4: Direct targeting of centrosomal pools of PKA or actin, alters the response to CXCL12**
859 a- Representative example of distribution of AKAP450, Pericentrin and F-Actin (visualized by specific
860 antibodies and phalloidin respectively). Scale bar = 10µm.
861 b- Left: Pretreatment with Ht31 peptide (AKAP II inhibitor), induces an increase of resting roundness
862 when compared with unstimulated CEM T cells incubated with the control peptide (Ht31P) (dotted
863 line). After 5 minute stimulation with CXCL12, the deformation observed in the presence of the
864 control peptide, is abolished when AKAP II inhibitor is present. Mean ± SE of 5 independent
865 experiments, 280-3589 cells/condition/experiment.
866 Right: Pretreatment with the AKAP II inhibitor peptide Ht31, induces an increase of resting
867 centrosomal actin when compared with unstimulated CEM T cells incubated with the control peptide
868 (Ht31P) (dotted line). After 5 minute stimulation with CXCL12, this content remains above the level
869 measured with the control peptide when AKAP II inhibitor is present. For each experiment, values
870 have been normalized relatively to the mean intensity of centrosomal F-actin measured in
871 unstimulated cells treated with Ht31-P (control peptide). Mean ± SE of 5 independent experiments.
872 30-70 cells/condition/experiment.
873 c- The levels of actin (left, phalloidin labeling) and microtubules (right, anti-α-tubulin labeling) were
874 measured concomitantly in CEM T cells in control conditions, after CXCL12 stimulation or H89

875 pretreatment. For each experiment, values have been normalized relatively to the mean intensity of
876 centrosomal F-actin or α-tubulin measured in untreated and unstimulated cells. Mean ± SE of 4
877 independent experiments, 29-150 cells/condition/experiment.
878 d- Example of simultaneous recording of cell roundness (blue line) and centrosomal actin (black line)
879 in a LifeAct-mCherry-transfected CEM T cell, upon CXCL12 stimulation (black arrow). The gray arrow
880 indicates the time between decreases of centrosomal actin and cell roundness. Red arrow: level of
881 centrosomal actin at which the cell starts to deform.
882 e- Centrin1-VCA expressing CEM T cells present higher level of centrosomal actin (left) and increase
883 of cell roundess (right) compared to Centrin1 expressing cells. In these cells, the effect of CXCL12 is
884 reduced. Left panel: for each experiment, values have been normalized relatively to the mean
885 intensity of centrosomal F-actin measured in unstimulated centrin1-transfected CEM T cells. Mean ±
886 SE of 6 independent experiments, 19-69 cells/condition/experiment (left). Mean ± SE of 7
887 independent experiments, 103-437 cells/condition/experiment (right).
888
889 **Figure 5: Link between PKA, centrosomal actin and cell roundness**
890 a- Correlation between centrosomal actin and cell shape. For the different conditions and for a given
891 cell, centrosomal actin level and roundness have been normalized to the mean values of the control
892 cells of the same experiment. Each dot represents the average ± SE of 86-359 individual cells.
893 b- Summary of the sequence of events leading to cell polarization after CXCL12 stimulation.
894 Calcium/cAMP/PKA variations are displayed in parallel to cytoskeleton reorganization.
895

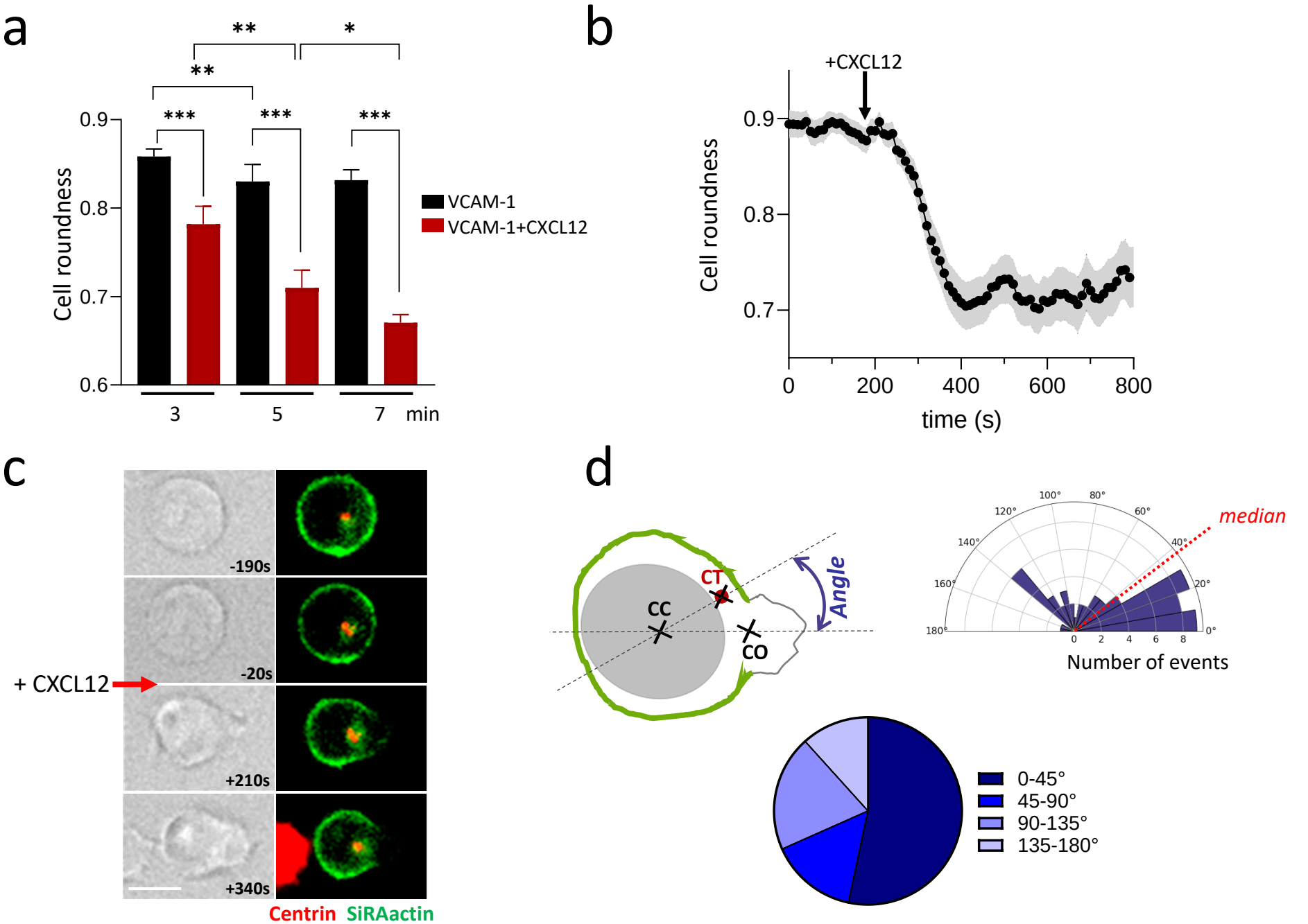
a
**
*
**
***
***
***
0.9
0.8
0.7
0.6
Cell roundness
VCAM-1
VCAM-1+CXCL12
3
5
7
min
b
+CXCL12
0.9
0.8
0.7
Cell roundness
0
200
400
600
800
time (s)
c
-190s
-20s
+ CXCL12
+210s
+340s
Centrin
SiRAactin
d
CT
CC
CO
Angle
median
100°
80°
120°
60°
140°
40°
160°
20°
180°
0°
0
2
4
6
8
Number of events
0-45°
45-90°
90-135°
135-180°

Figure 1

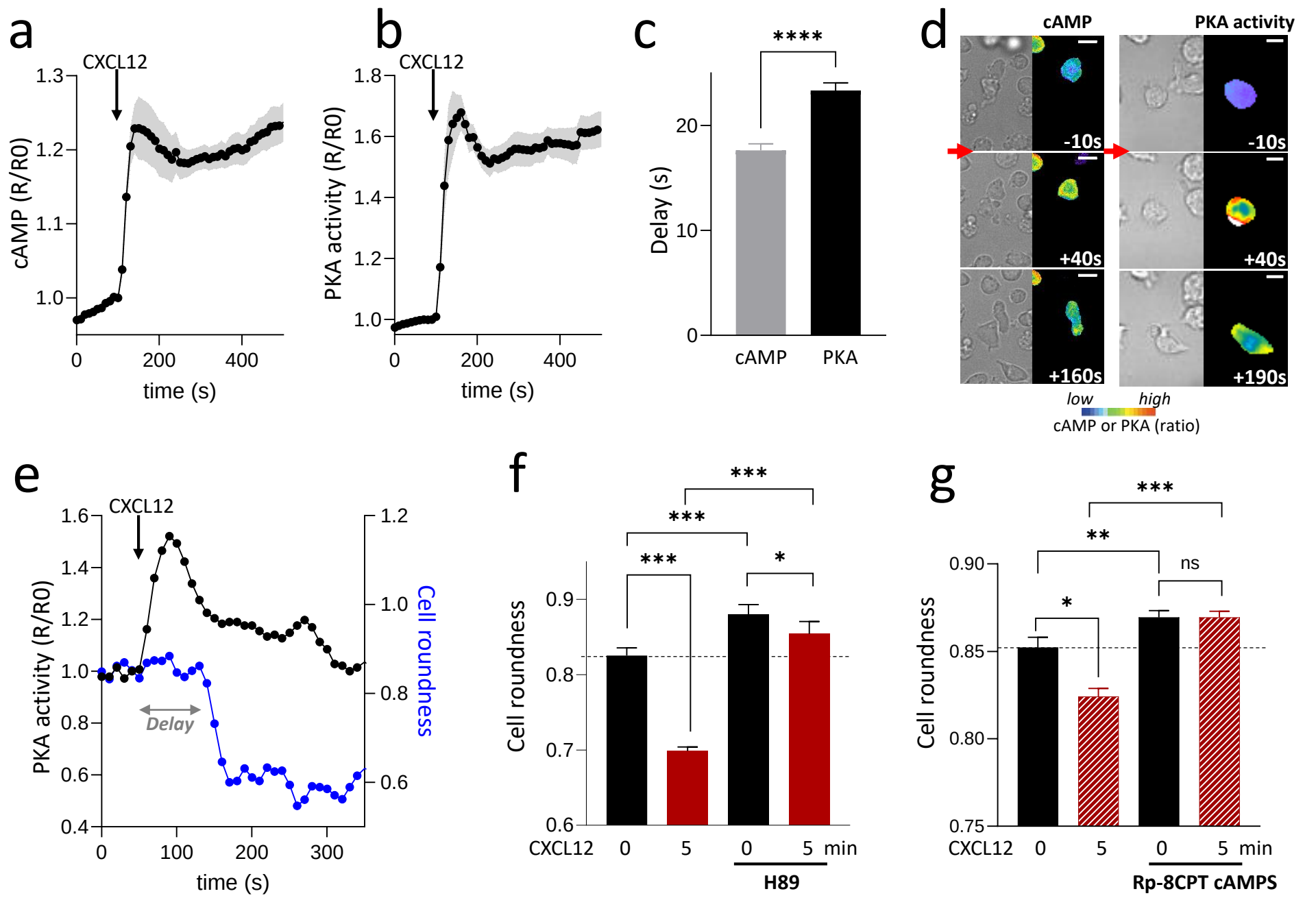
a
CXCL12
cAMP (R/R0)
time (s)
b
CXCL12
PKA activity (R/R0)
time (s)
c
****
Delay (s)
cAMP
PKA
d
cAMP
PKA activity
-10s
+40s
+160s
+190s
low
high
cAMP or PKA (ratio)
e
CXCL12
PKA activity (R/R0)
Cell roundness
Delay
time (s)
f
***
***
***
*
Cell roundness
CXCL12 0 5 0 5 min
H89
g
***
**
*
ns
Cell roundness
CXCL12 0 5 0 5 min
Rp-8CPT cAMPS

Figure 2

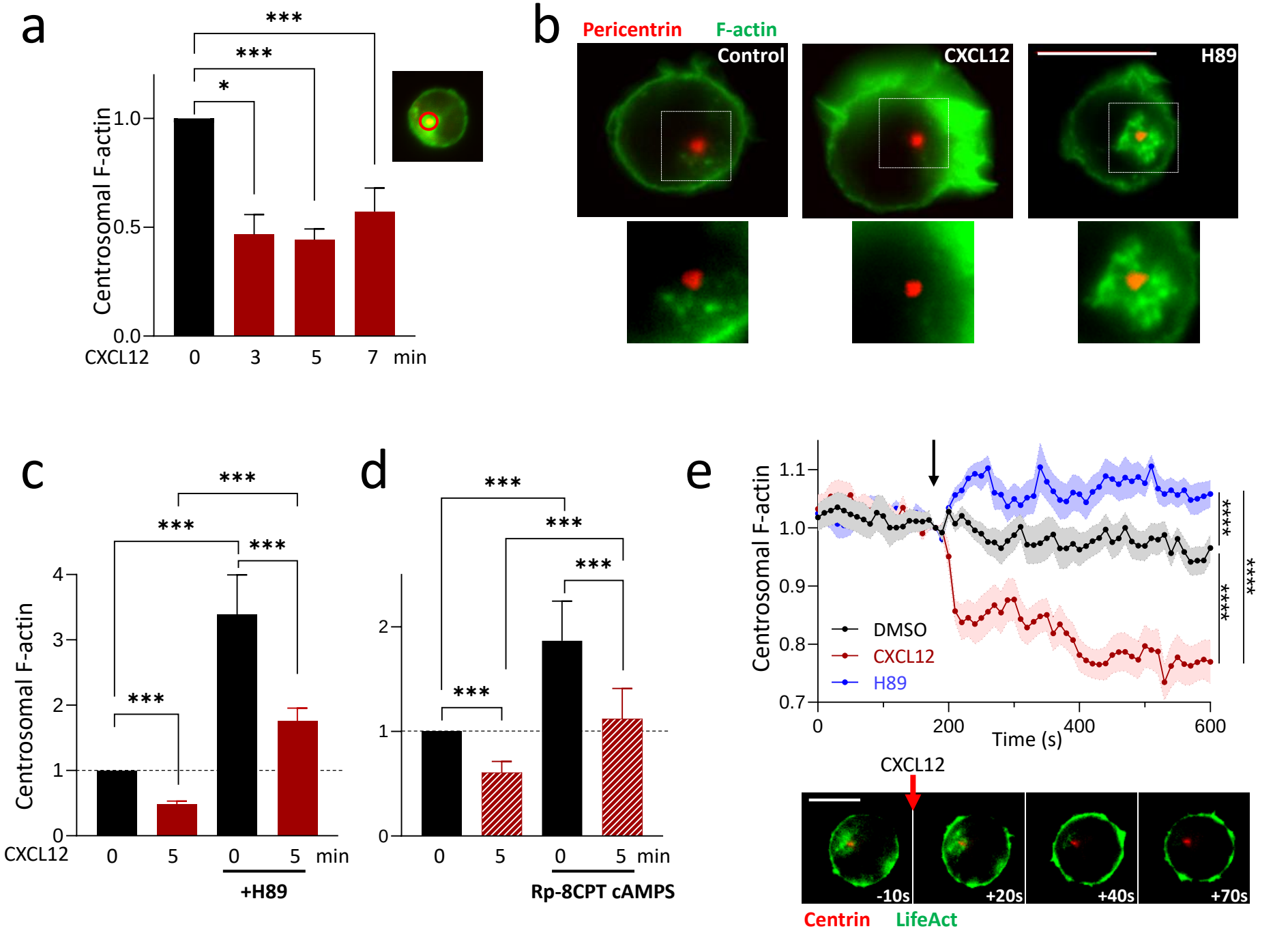
a
Centrosomal F-actin
1.0
0.5
0.0
CXCL12
0
3
5
7
min
***
***
*
b
Pericentrin
F-actin
Control
CXCL12
H89
c
Centrosomal F-actin
4
3
2
1
0
CXCL12
0
5
0
5
min
+H89
***
***
***
***
d
Centrosomal F-actin
2
1
0
0
5
0
5
min
Rp-8CPT cAMPS
***
***
***
***
e
Centrosomal F-actin
1.1
1.0
0.9
0.8
0.7
0
200
400
600
Time (s)
DMSO
CXCL12
H89
****
****
****
CXCL12
-10s
+20s
+40s
+70s
Centrin
LifeAct

Figure 3

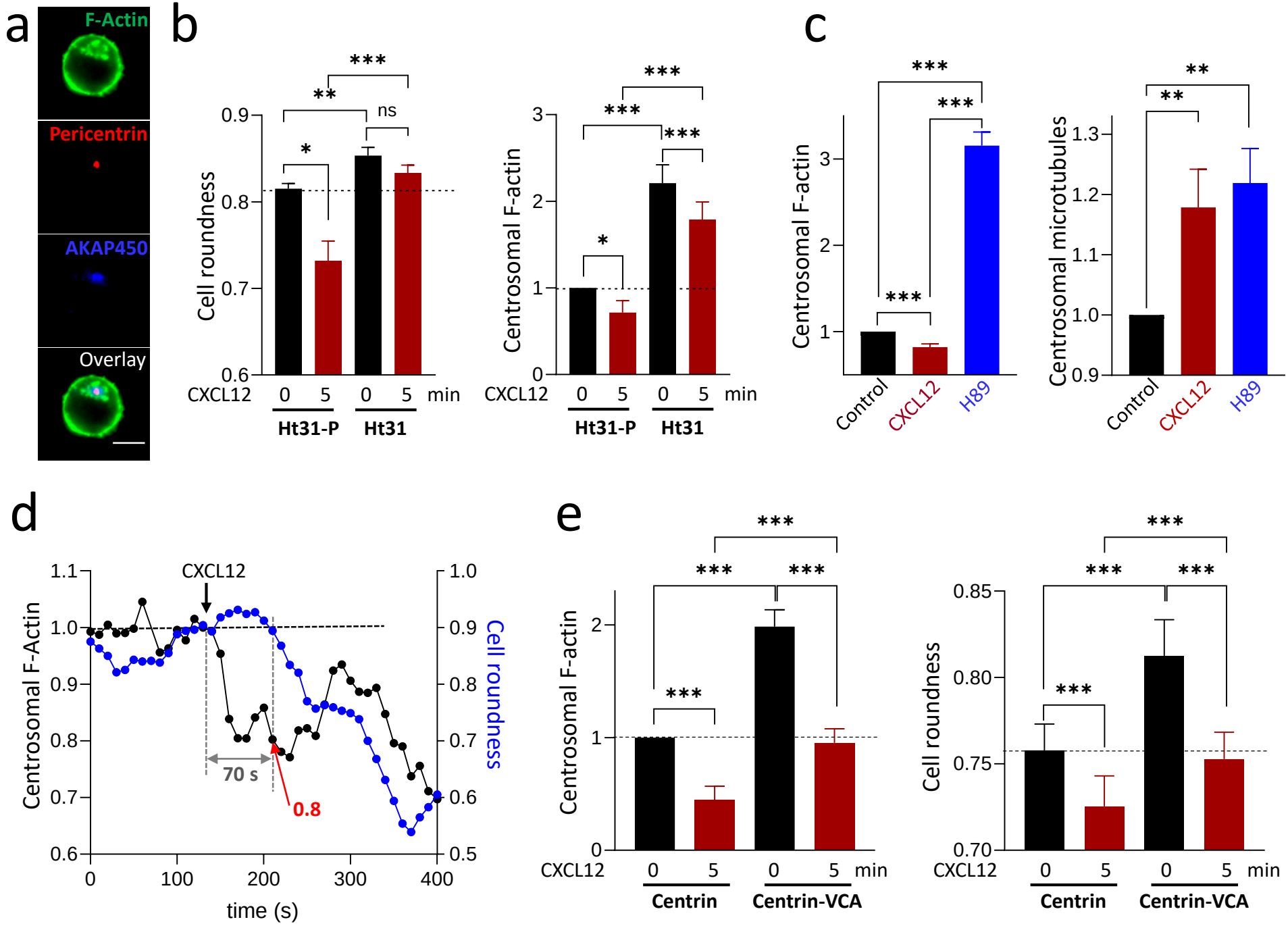
a
F-Actin
Pericentrin
AKAP450
Overlay
b
Cell roundness
CXCL12
0 5 0 5 min
Ht31-P
Ht31
ns
Centrosomal F-actin
c
Centrosomal F-actin
Centrosomal microtubules
Control
CXCL12
H89
d
CXCL12
Centrosomal F-Actin
Cell roundness
70 s
0.8
time (s)
e
Centrosomal F-actin
Cell roundness
Centrin
Centrin-VCA

Figure 4

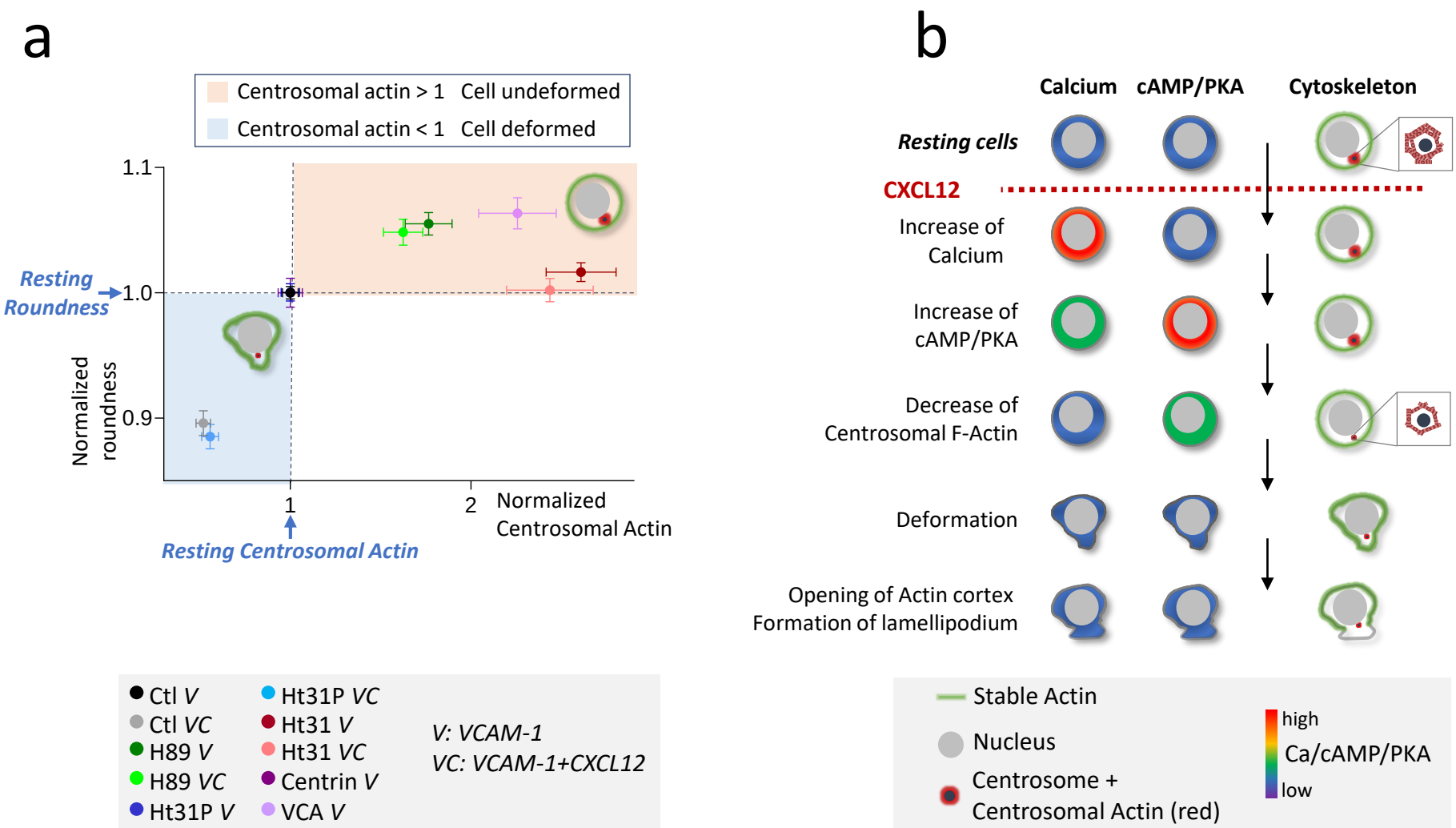
a
Centrosomal actin > 1 Cell undeformed
Centrosomal actin < 1 Cell deformed
1.1
1.0
0.9
Resting Roundness
Normalized roundness
1
2
Normalized Centrosomal Actin
Resting Centrosomal Actin
Ctl V
Ctl VC
H89 V
H89 VC
Ht31P V
Ht31P VC
Ht31 V
Ht31 VC
Centrin V
VCA V
V: VCAM-1
VC: VCAM-1+CXCL12
b
Calcium
cAMP/PKA
Cytoskeleton
Resting cells
CXCL12
Increase of Calcium
Increase of cAMP/PKA
Decrease of Centrosomal F-Actin
Deformation
Opening of Actin cortex
Formation of lamellipodium
Stable Actin
Nucleus
Centrosome + Centrosomal Actin (red)
high
Ca/cAMP/PKA
low

Figure 5

Supplementary figure legends

Figure Supp 1: Distribution of CXCR4 in unstimulated and stimulated cells.

Example of CXCR4 distribution revealed by immunofluorescence in 8 different unstimulated (left) and 5 different CXCL12-stimulated (right) CEM T cells. The centrosome is labelled with an antibody against pericentrin (green).

Scale bar = 10µm.

Figure Supp 2: Calcium and cAMP variations upon CXCL12 stimulation

a- Simultaneous measurements of Ca and cAMP variations in CEM T cells transfected with TEpacVV and loaded with Fura-2. CXCL12 stimulation is indicated by the black arrow. For both parameters, values have been normalized relatively to the value at the time of stimulation. Mean ± SE of 13 cells.

b- CXCL12-induced cAMP variations in CEM T cells transfected with TEpacVV and preincubated or not with the Ca chelator BAPTA/AM. Values have been normalized relatively to the Ca value at the time of stimulation. Mean ± SE of 5 independent experiments, 6-19 cells/condition/experiment.

Figure Supp 3: Involvement of PKA in CXCL12-induced CEM T cell deformation and migration

a- Example of morphology of CEM T cell stimulated or not with CXCL12 and with or without pretreatment with H89. F-Actin (green) has been labelled with Phalloidin. Scale bar = 20µm.

b- Transwell migration assay with CEM T cells pretreated or not with H89. When indicated, CXCL12 was added to the lower compartment. Mean ± SE of 3 independent experiments.

Figure Supp 4: Sensitivity of CXCL12-stimulated human Primary Blood T cells to PKA inhibitor

a- Example of morphology of PBT stimulated or not with CXCL12 and with or without pretreatment with H89. F-Actin (green) has been labelled with Phalloidin. Scale bar = 20µm.

25 b- Quantification of cell roundness of PBT stimulated or not with CXCL12 and with or without
26 pretreatment with H89. Mean ± SE of 4 independent experiments (4 different donors), 64-871
27 cells/condition/experiment.
28 c- Example of F-actin distribution in PBT stimulated or not with CXCL12 and with or without
29 pretreatment with H89. F-actin is labeled with Phalloidin (green) and centrosome with an antibody
30 against pericentrin (red). Scale bar = 20µm.
31 d- Quantification of centrosomal actin in PBT stimulated or not with CXCL12 and with or without
32 pretreatment with H89. For each experiment, values have been normalized relatively to the mean
33 intensity of centrosomal F-actin measured in unstimulated and untreated PBT. Mean ± SE of 4
34 independent experiments (4 different donors), 11-57 cells/condition/experiment.
35
36 **Figure Supp 5: Effect of Rp-8CPT cAMPS on cell roundness and centrosomal actin level**
37 a- Cell roundness of CEM T cells pretreated or not with Rp-8CPT-cAMPS and deposited on VCAM-1 or
38 VCAM1+CXCL12 (1µg/ml) for 5 minutes. Mean ± SE of 4 independent experiments, 500-1226
39 cells/condition/experiment.
40 b- Centrosomal actin measured in CEM T cells pretreated or not with Rp-8CPT-cAMPS and stimulated
41 or not with CXCL12 (100 ng/ml) for 5 minutes. For each experiment, values have been normalized
42 relatively to the mean intensity of centrosomal F-actin measured in unstimulated and untreated CEM
43 T cells. Mean ± SE of 3 independent experiments, 26-61 cells/condition/experiment.
44
45 **Figure Supp 6: Effect of CXCL12 and PKA inhibition on centrosomal Arp2 and F-Actin distribution**
46 a- Example of F-Actin and Arp2 distributions in representative CEM T cells in control conditions (upper
47 line), after CXCL12 stimulation (middle line) or after H89 pretreatment (lower line). Scale bar = 10µm.
48 b- Effect of CXCL12 stimulation and PKA inhibition (H89) on F-Actin and Arp2/3 intensities at the
49 centrosome. The quantification of the two proteins have been performed on the same cells. For each
50 experiment and for both proteins, values have been normalized relatively to the mean intensity

measured in unstimulated and untreated CEM T cells. Mean ± SE of 4 independent experiments, 38-165 cells/condition/experiment.

Figure Supp7: Effect of the AKAP II Inhibitor Ht31 on the distribution of PKA catalytic subunit

a- Example of PKA Cα distribution in CEM T cells treated with control peptide (Ht31-P) or with AKAP II inhibitor, Ht31. F-Actin labeled with phalloidin (green) and centrosome revealed with an antibody against pericentrin (red). Scale bar: 10µm.

b- Ratio between PKA Cα intensities measured in a 3µm diameter area centered at the centrosome with the ones measured in a similar area in the cytoplasm in cells either treated with the control peptide (Ht31-P) or with the AKAP II inhibitor (Ht31). A ratio >1 reflects an accumulation of the protein around the centrosome. Mean ± SE of 3 independent experiments, 12-95 cells/condition/experiment.

Figure Supp 8: Effect of Centri1-VCA expression on cell morphology and actin distribution

a- Example of F-actin distribution (green) in CEM T cells transfected with either centrin1-GFP or with centrin1-VCA-GFP (magenta). The centrosome is revealed with an antibody against pericentrin (red). Scale bar = 10µm.

b- Example of morphology of CEM T cell transfected with either centrin1-GFP or with centrin1-VCA-GFP. F-actin is labelled with phalloidin (green). Scale bar: 10µm

Figure Supp 9: F-Actin and α-tubulin in CEM T cells

Examples of cytoskeleton distribution in CEM T cells in control conditions, stimulated with CXCL12 or pretreated with H89. F-Actin (green) is labelled with phalloidin, the centrosome with anti-pericentrin antibody and microtubules with anti-α tubulin antibody. Scale bar = 10µm.

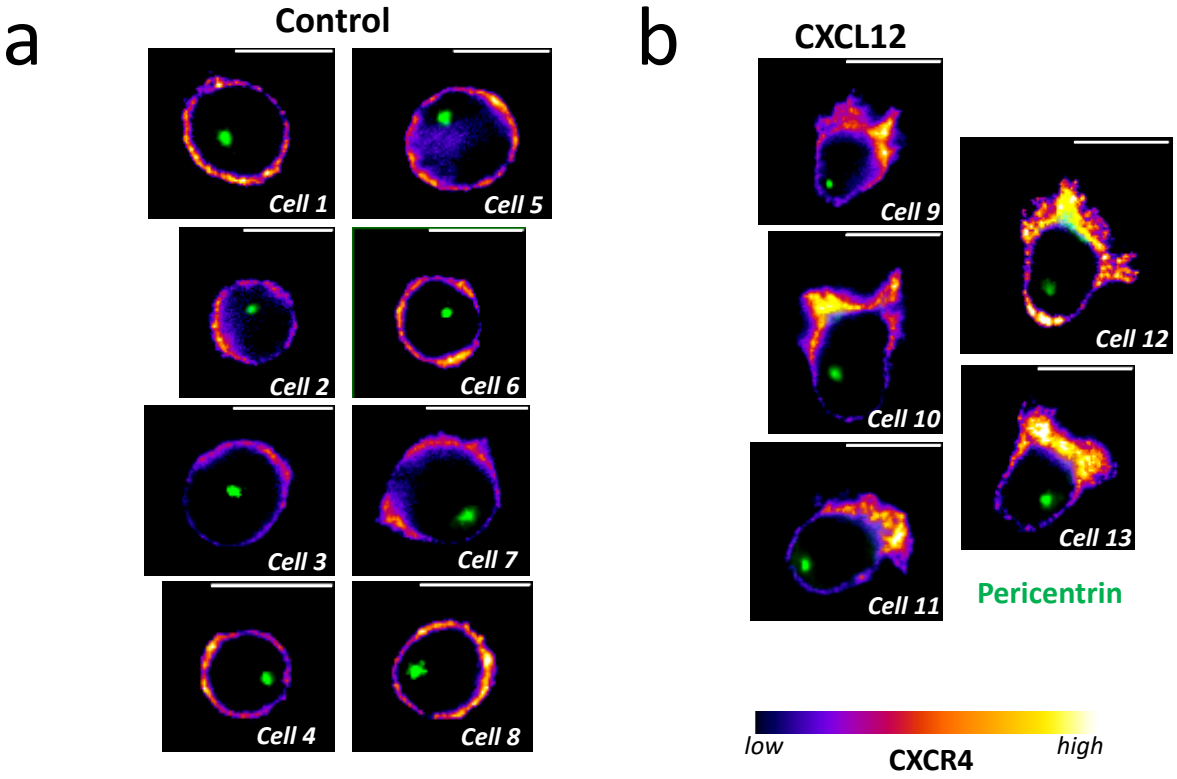

Figure Supp 1

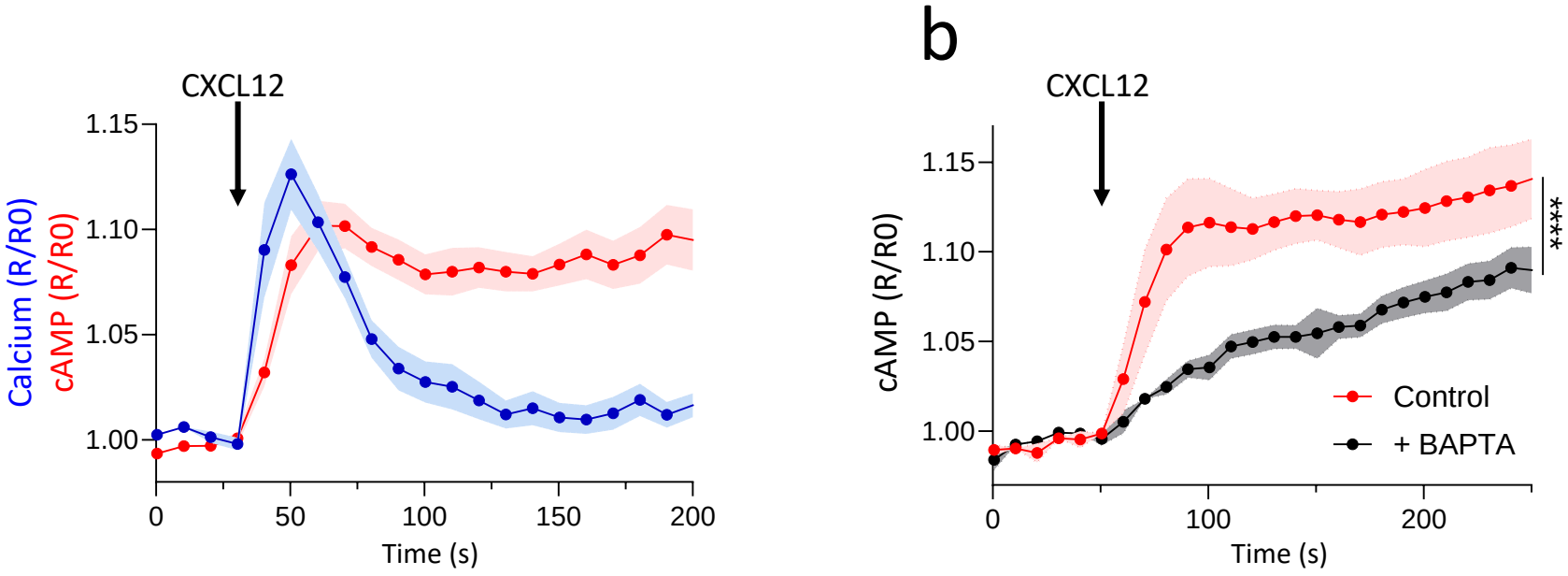

Figure Supp 2

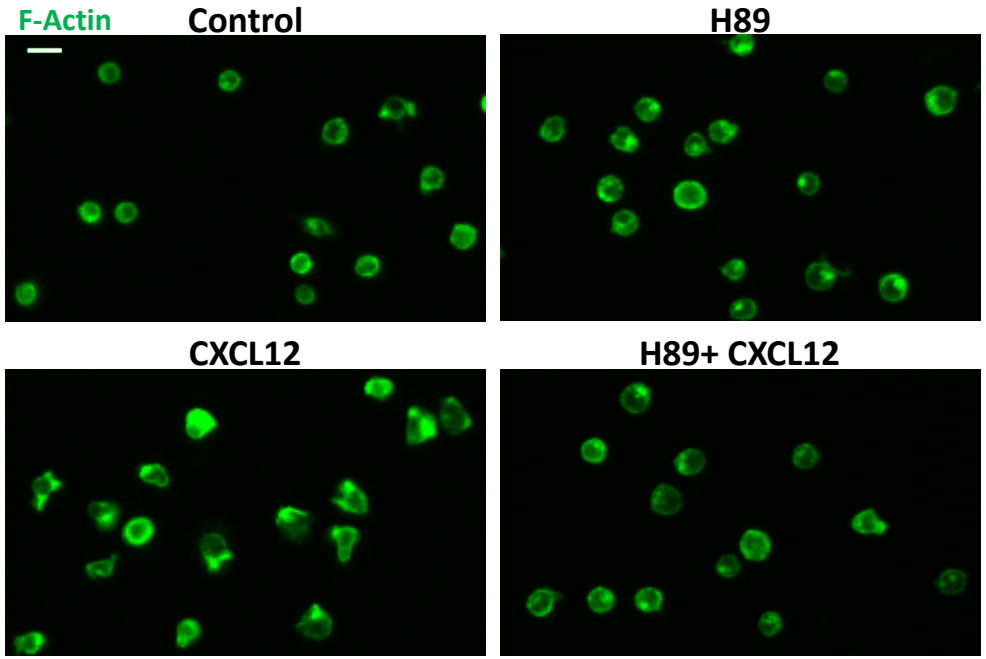

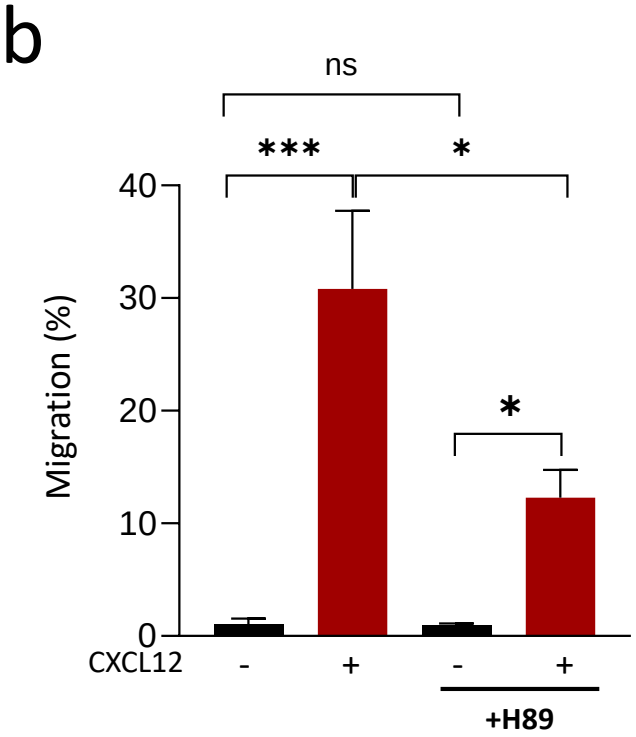

Figure Supp 3

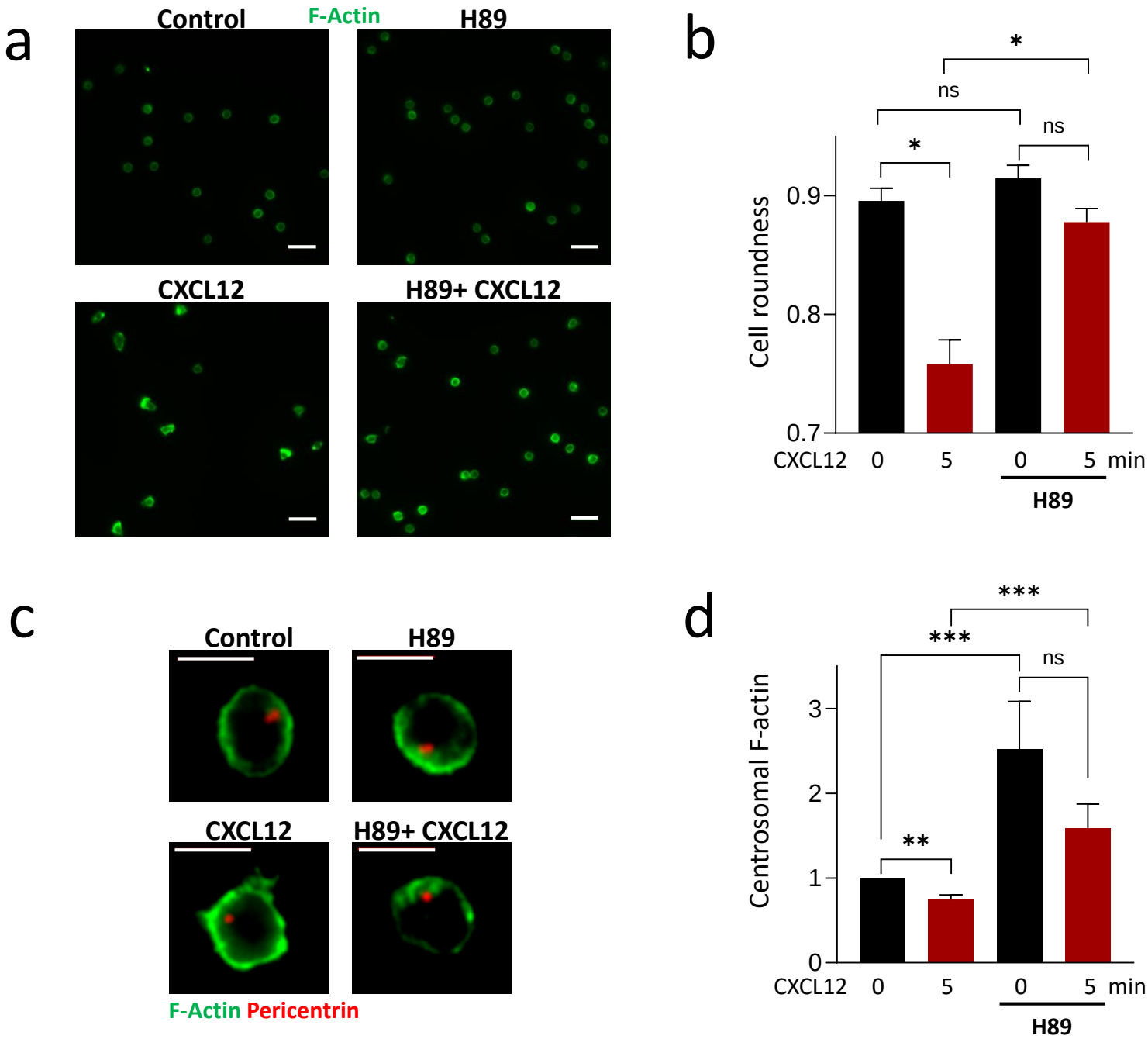

Figure Supp 4

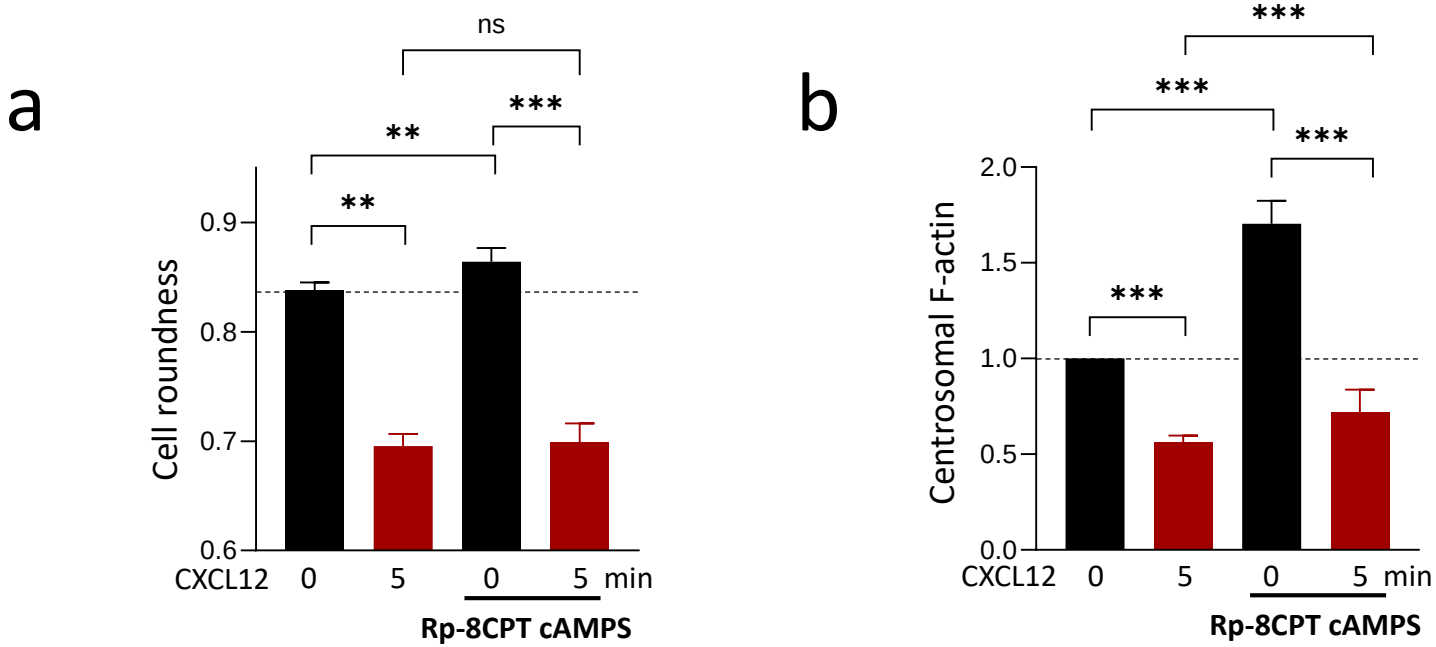

Figure Supp 5

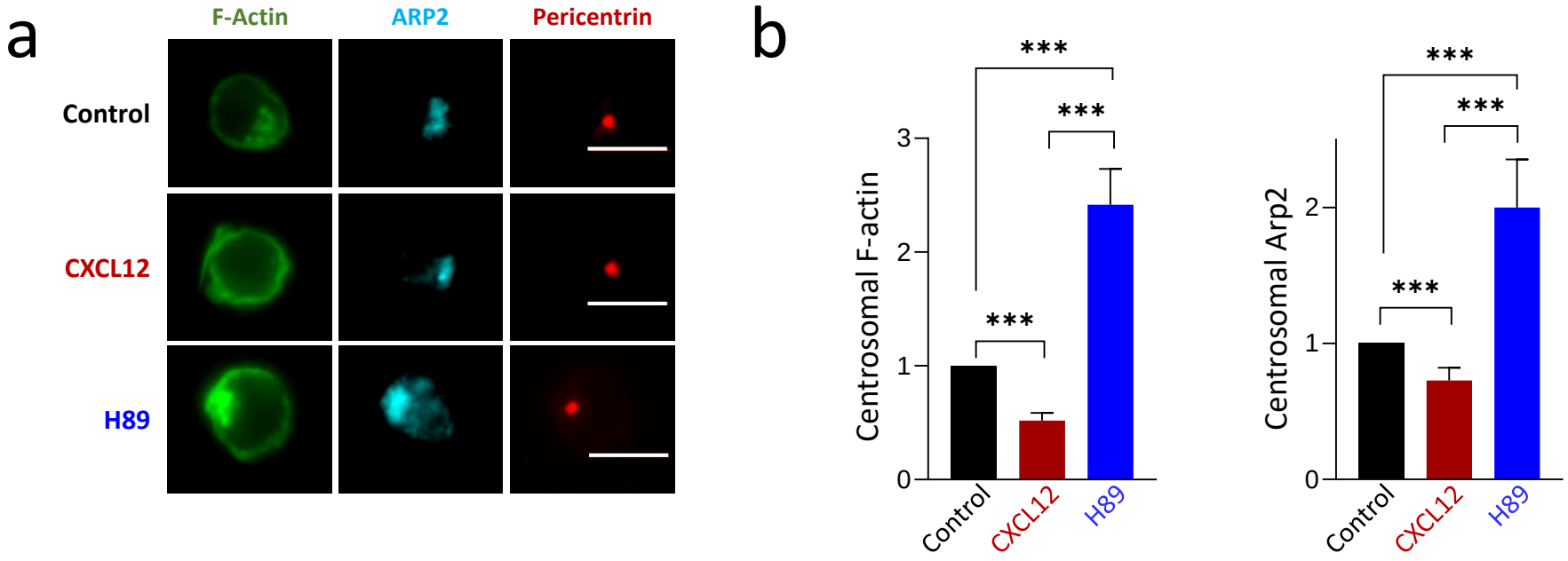

Figure Supp 6

a

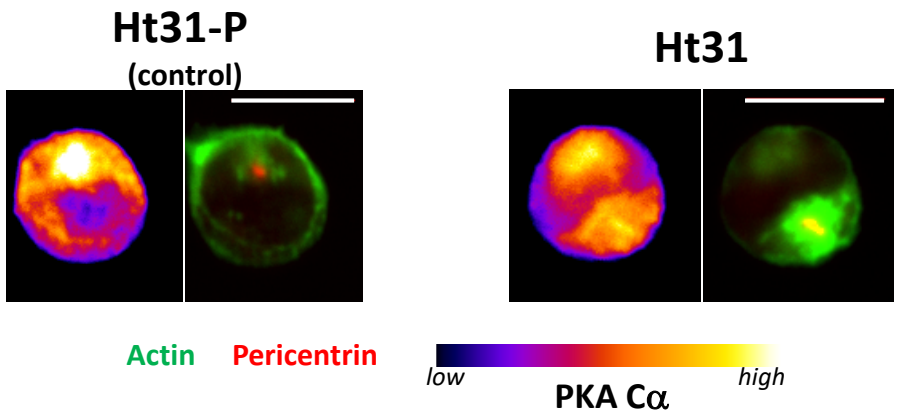

b

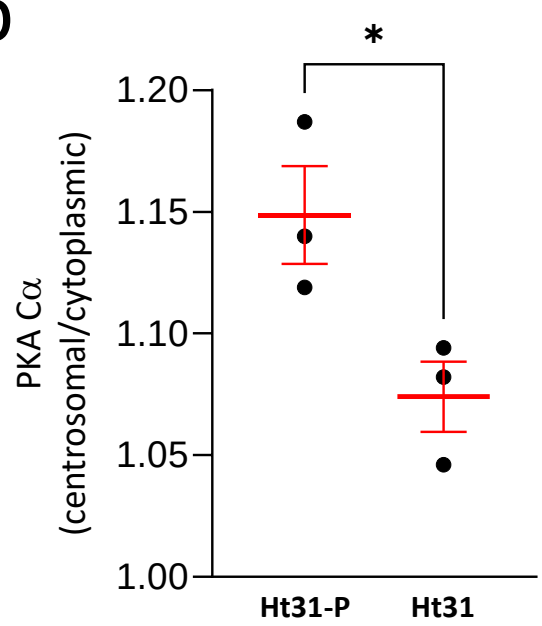

Figure Supp 7

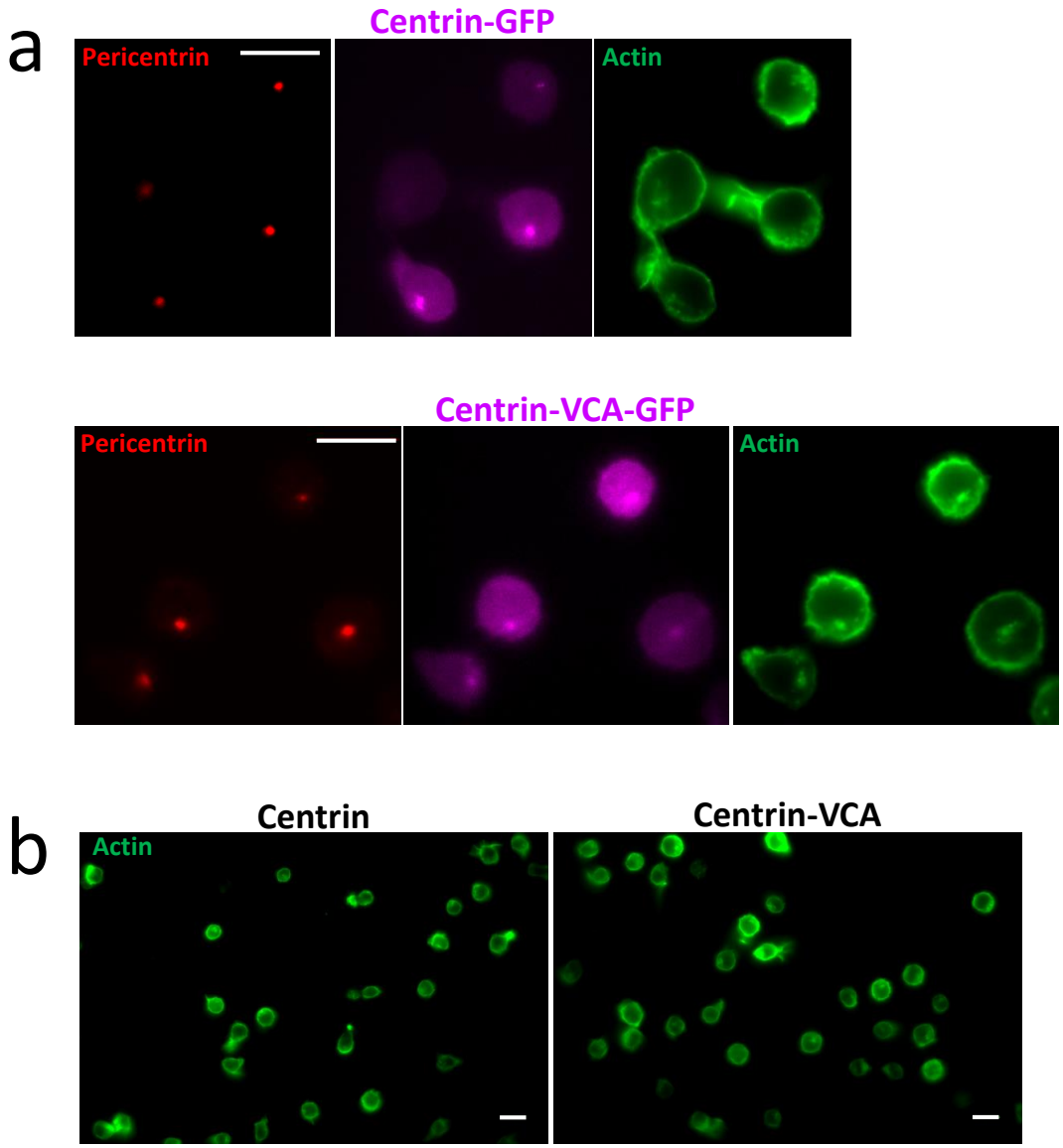

Figure Supp 8

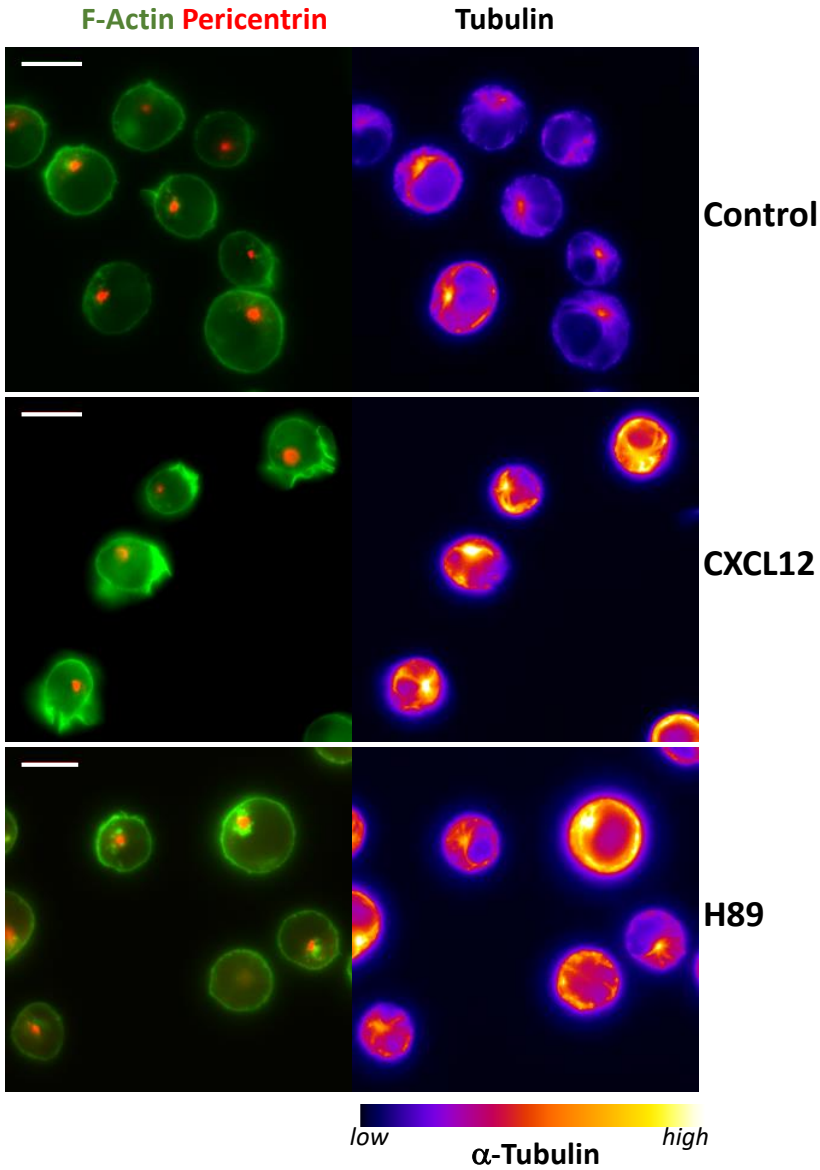

Figure Supp 9

Full Revision

Manuscript number: RC-2024-02542
Corresponding author(s): Clotilde, Randriamampita

1. General Statements [optional]

2. Point-by-point description of the revisions

Reviewer #1

The limitation I see is the use of a single cell line system of cancerous origin and the fact that only changes in cellular morphology are quantified, but not cellular behavior itself - e.g migration, T cell intrinsic signalling. If some key observations can be validated in primary T cells this would be perfect, or at least in a second model system. If signalling related to changed morphology is affect by regional inhibition of PKA/actin remodelling, remains uncertain, too - maybe there is a way to monitor additional parameters, other than roundness/PKA activity.

- In order to complete our results, key experiments have been performed in primary human blood T lymphocytes (PBT). 4 experiments have been realized with 4 different donors. In this model, as in CEM T cell line, we have observed that:

- chemokine-induced PBT deformation is inhibited by the PKA inhibitor H89. Unstimulated PBT are poorly deformed so that H89 by itself only slightly (but not significantly) increases resting roundness.

- chemokine stimulation induces a decrease of centrosomal actin which is partly prevented by H89 treatment. In these conditions, centrosomal actin remains at a level superior to the resting one. H89 by itself is sufficient to promote an increase in centrosomal actin.

Altogether, these results demonstrate that in PBT as in CEM, in resting conditions as well as after chemokine stimulation, the level of centrosomal actin is controlled by PKA activity and is associated with cell deformation.

These new results are presented in Fig Supp 4 and described in the manuscript (lines 158-164 and 199-202).

- In order to investigate the consequences of the PKA inhibition on chemokine-induced cell behavior, Transwell migratory assays have been performed. As presented in Fig Supp 3b, the chemokine-triggered T cell migration through 5µm pores is reduced by H89 pretreatment. This suggests that the reduction of T cell deformation after PKA inhibition has a direct consequence on the physiological behavior of T lymphocyte. This result is described in the manuscript (lines 165-169).

Reviewer #2

Major points:

(i) Many experimental microscopy datasets are quantified but lack representative images. These representative images are important to be able to judge the underlying data and should be

included for the datasets shown in Figure 2, Fig. 3c, Fig. 4d (Lifeact examples), and Fig. 6 (Centrin VCA). In addition, the differences in the signal intensity of the actin cytoskeleton are sometimes hardly visible in the provided representative images (e.g., Fig. 4b, control vs CXCL12). Could the authors come up with solutions to show this in a better way (e.g., zooms and/or fire-colour coding)?

As suggested by the reviewer, some representative images have been added for all experiments (Figures 3, Supp 3a, Supp 4 a & c, Supp 7a, Supp 8). Furthermore, a zoom of actin network around the centrosome in different conditions is now presented in Fig 3b (previous Fig 4b)).

(ii) The authors use an experimental setup in which the cells 'see' a homogenous chemokine concentration around them. Further, they discuss different models in the introduction of how the local cellular polarisation in such a uniform chemokine sounding is defined, including a model of polarised localisation of chemokine receptors on the plasma membrane. However, in a tissue, chemokines are typically not homogeneously distributed but are present in the form of a gradient, e.g. due to local chemokine sources or the self-generation of chemotactic gradients by neighbouring migrating cells. Therefore, it would be interesting to know whether the described repositioning of the centrosome and the changes in the actin pool are also important if cells are in a chemokine gradient. Experimentally, this could be addressed by providing a local chemokine source (e.g. from a micropipette). If this goes beyond the scope of the manuscript, then at least this aspect of chemokine gradients should be clearly mentioned and discussed in the introduction and the discussion sections.

We thank the reviewer for this remark. We had not actually addressed this point.

- We have tried to create chemokine gradients. But, we have never been able to observe all cells polarizing in the same direction (along this gradient). This negative result might however be due to our experimental setup so that this result is not mentioned in the manuscript. However, to our knowledge, no real chemotaxis has been described in T lymphocytes.
- We have performed some Transwell assays that mimic trans-endothelial migration and have shown the involvement of PKA (Figure Supp 3b, lines 165-169). But the involvement of centrosomal actin could not be investigated in this experiment.
- This question is now addressed in introduction (lines 44-47) and in discussion (lines 400-405).

(iii) Given that the centrosome acts as a microtubule-organising center (MTOC), it would be interesting to see the microtubules during polarisation. Did the author try the visualisation of microtubules in live or by immunofluorescence stainings? Would it be a plausible model that reduced actin polarisation allows microtubule polarisation towards the cell periphery and thereby induces a protrusion by delivering signalling and cytoskeleton components towards the newly forming protrusion? May this be only targeted towards one side of the centrosome, as the nucleus may sterically hinder the efficient growth of microtubules to the other cellular side? What would happen in cells without a nucleus? And what would happen in cells without a centrosome (e.g., by PLK4 inhibition via centrinone) - are cells still able to form protrusions efficiently? These experimental suggestion are optional but could significantly improve the study.

- As suggested by the reviewer, we performed new experiments to quantify microtubules together with actin in the centrosomal area. As previously mentioned in discussion, we were

expecting that microtubule evolution mirrors that of actin. This is indeed the case after chemokine stimulation, where the quantity of microtubules present in the centrosomal area increases as actin decreases. However, after H89 treatment, an enrichment of both cytoskeleton networks is observed. It suggests that PKA could affect directly microtubule polymerization/depolymerization equilibrium independently of actin level possibly through Microtubules Associated proteins phosphorylation. Nevertheless, the effect of centrosomal actin level on cell polarization we emphasize, might partly be due to its consequence on microtubule growth.
These results are now presented in Figure 4c and representative images shown in Figure Supp 9. Furthermore, this observation is mentioned in the results part (line 256-263) and in discussion (line 428-442).

- The sterical role of the nucleus on the polarization is an interesting hypothesis that we have been however unable to test it. T lymphocytes are small cells (around 15µm diameter for CEM cell line) that seems to be difficult to enucleate.
- We have tried to obtain cells without centrosomes in order to test their ability to polarize. To this purpose, we have treated cells with the PLK4 inhibitor, centrinone (500nM) for 24 to 48h hours. Although we could observe after 33 hours, that the large majority of cells present only one centriole, we never got cells without centrioles. After this one-centriole stage, the cells started dying.

(iv) Bringing actin artificially to the centrosome via the centrin-VCA construct is a very nice approach. However, the dataset would strongly benefit from samples, in which the chemokine CXCL12 is included.
The effect of chemokine on centrin-VCA expressing cells has been investigated. This result is displayed in Fig 4e. In cells expressing the centrin-VCA construct, the level of actin at the centrosome is higher than in control cells. However, upon chemokine stimulation, the signaling pathways leading to actin reduction are still active so that the level of centrosomal actin decreases (insignificantly different to the control) and the cells do not deform (insignificantly different to the control). These results are now discussed in the manuscript (lines 283-287).

Minor points:
(i) The study is based on a lymphoblastic cell line called CEM T cells. This should be clearly stated at the beginning of the results section and in all figure legends, as it remains unknown whether primary T lymphocytes would show the same behavior. Additionally, the methods section should contain more details about this cell line, e.g. whether it is from mouse or human origin.
The cells used for the experiments are now clearly indicated in the figure legends and specifed in the manuscript (results and methods).
Furthermore, as mentioned in the response to reviewer #1, new experiments have been performed with primary human blood T cells. Similar effect of PKA on cell deformation and centrosomal actin regulation have been observed. These new experiments are presented in Fig Supp 4 and described in the manuscript (lines 158-164 and 199-202).

(ii) The authors mention 'suboptimal' conditions of stimulation. However, it remains unclear in the results sections what this means. Some of the experimental modulations (e.g. the cAMP analog

Rp-8-CT-cAMPS) seem to only show an effect in these suboptimal conditions but not in the optimal conditions. This should be clearly stated and discussed.

In resting cells, Rp-8-CT-cAMPS has a similar effect as H89: it induces an increase in cell roundness as well as in centrosomal actin. However, after chemokine simulation, the inhibition of cell deformation and of centrosomal actin reduction is only observed with low intensity stimulation (Figures 2g & 3d *vs* Supp 5a). Our interpretation is that this chemical is not potent enough to counteract strong activation of PKA. Indeed, in resting conditions or after mild PKA activation, it blocks the effect of chemokine. This might be due to the fact that the inhibitor concentration reached within the cells is not enough. The text concerning this part has been modified for more clarity (lines 171-178 and 203-206) and the figure legends mention explicitly the chemokine concentrations used for stimulation.

(iii) 23 out of the 38 references are older than 5 years, and most of them are older than 10 years. While it is surely very important to refer to these older findings, the authors may include more knowledge from recent years. This may include references about centrosome positioning in immune cells and motile cells (e.g., PMID32379884, PMID29934494, PMID30944468, PMID37987147, PMID36398880, PMID38627564, PMID33634136) and the actin cytoskeleton at the centrosome (PMID33609453), PMID33184056, PMID36111670.

The references have been updated and more recent publications added.

(iv) The first paragraph of the discussion (lines 253 - 262) needs references.

Some references have been added to this paragraph.

(v) Some Figures maybe combined as the findings are closely related (e.g., Figures 2 and 3; and Figures 5 and 6).

The figures have been modified according to this suggestion.

(vi) Line 94, Supply. Fig. 1: the authors that the chemokine receptor CXCR4 has a uniform distribution in non-stimulated cells. This is not directly evident in the images as there are areas of more and less signal. It would be important to clearly describe this in the text. Further, the labelling of the figure would benefit from labelings such as 'cell 1', 'cell 2', etc to directly make clear that these are images from 3 representative cells.

We thank the reviewer for this remark. The CXCR4 distribution is indeed not strictly uniform. We now use the fire-colour coding which makes this point more obvious in images (Fig Supp 1).

However, although some high spots of CXCR4 accumulation can be observed, they are not associated to the location of centrosome and, can thus not explain the preferential position of the polarization axis we observe. This point is discussed in the new version of the manuscript (lines 113-120).

Furthermore, in the new figure concerning CXCR4 distribution (Fig Supp 1), we labelled each image with " cell x" in order to explicit that this figure displays different representative cells.

(vii) Different centrin isoforms exist (centrin 1, 2, 3). It should be mentioned in the results and methods section, which isoform was used for their genetic constructs (e.g., centrin-GFP, centrin-VCA).
We have corrected this omission. The fact that centrin1 isoform was used is now mentioned in the text, the legends and in the methods part.

Reviewer #3

MAJOR COMMENTS
1. The authors state that "uniform CXCR4 labelling is observed in unstimulated cells" (ln94-95). While the panels in Supp Fig1a show a pattern in unstimulated cells that is obviously less dramatically asymmetrical than seen for stimulated (and, importantly, already polarized) cells in Supp Fig1b, the labelling in unstimulated cells is still far from uniform, as there is considerable heterogeneity of signal intensity along the perimeter. This is important, given that they are looking at a membrane receptor, even small fluctuations in which may be greatly amplified and thus have considerable effects on symmetry downstream. The authors should either quantify the intensity (e.g. signal as a function of polar coordinate value) or soften their language to more accurately reflect the data.
We thank the reviewer for this remark. The distribution of CXCR4 receptors is indeed not strictly uniform even in unstimulated cells. In order to make this point more obvious, we have used the fire-colour coding for CXCR4 distribution in Fig Supp1. As mentioned in the response to the reviewer #2, high spots of CXCR4 accumulation exist but they are not associated to the location of centrosome and thus, cannot explain the preferential position of the polarization axis we observe. This point is discussed in the new version of the manuscript (lines 113-120).

2. Regarding the analysis of polarization events in Fig. 1c and 1d, it is not clear how, exactly, the time point for the cortex opening is determined. For example, in the sample images in 1c, would the +110s or the +340s time point be used? The reason this is important is that the angle seems to change with time (at least in the example given) and there are also heterogeneities (specifically, decreases) in SiR-actin intensity along the cortex that precede cortex opening. Thus, it is not clear whether the cortex begins to open in closer proximity to the centrosome or whether the centrosome is further aligned after the cortex opens.
First of all, we would like to apologize that there is an error in the time labeling in Fig 1c. The third image corresponds to + 210s and not +110s. This has been corrected in the new Fig 1c. In this example, +210 s and not +340 s has been considered as the opening of the actin cortex.
More generally, the time for angle determination was performed by watching movies. Images were analyzed only relatively to previous and the next ones. Indeed, we first determined the period when 1/ SiRActin labeling stably decreases at one pole of the cell and 2/ the cell simultaneously deforms (transmitted light pictures). Playing the sequence backward, allowed us to determine the beginning of cortex opening. This time was then the reference for measuring the polarization

angles. Thus, transient SiRActin heterogeneities we could indeed observe sometimes, were not considered. These precisions have been added to the Methods section (lines 559-564)

3. Also regarding Figure 1d, it is not clear how many cells and experimental replicates are represented in the data - the Results text reports 60 cells from 11 experiments (ln106) but the legend reports 58 cells (ln564) without mention of experimental replicate number.
We thank the reviewer for pointing out this error which we have corrected. The correct number of cells is 60. These cells are from 11 different experiments. We pooled all individual values of the 60 cells to establish angle distribution.

Also, while the rose plot is useful, it is important to have statistical analysis on the skewness of the response and/or to report something other than the average angle - for example, the percentage of cells with a cortex opening in the same 90-degree quadrant as the centrosome.
For more clarity, the position of the median has been added to the rose plot. Furthermore, a pie plot reports now the distribution of the angles (Fig 1d).

Finally, it might be clearer to the reader to have the rose plot and the model cell oriented in the same direction.
We agree to this suggestion and the cell (Fig 1c), the schematic drawing and the rose plot (Fig 1d) are all three oriented in the same direction.

4. For their PKA inhibition experiments, the authors introduce H89 as "a competitive inhibitor of ATP on the PKA catalytic subunit" (ln138-139). H89 is a very non-specific inhibitor, as demonstrated by Davies et al (PMID 10998351) and reviewed by Lochner & Moolman (PMID 17214602) and should be introduced more accurately.
H89, as a competitive inhibitor of ATP, is indeed not specific to PKA. At the low concentration we used, few other kinases can be inhibited. We now introduce more precisely the inhibitor and add references (lines 152-155 and 172-173).

To their credit, the authors use an orthogonal approach of PKA inhibition with a cAMP analog and see comparable effects. Those data, currently in Supp Fig. 3, should be included as primary data, given that the H89 data can only be correctly interpreted in the context of the Rp-cAMPS data (this applies to both Fig3 and Fig4).
As suggested, the data concerning Rp-8CPT-cAMPS are now included in the main figures (Fig 2g & Fig 3d) and the text has also been modified (lines 172-178 and 203-206).

5. As part of Fig.5, the authors state "AKAP450 is a type II AKAP i.e. it is able to bind RII subunits of PKA. In order to determine whether this AKAP allows a [sic] compartmentalization of the PKA activity responsible for centrosomal F-actin regulation, we used the specific peptide (Ht31)". Ht31 broadly inhibits PKA anchoring; its effect is not specific for any individual AKAP, including AKAP9/AKAP450.
We completely agree with this point and did not want to mean that Ht31 was specific to AKAP450. Therefore, the sentence has been modified to be more explicit (lines 234-236).

Moreover, the authors neither show/confirm PKA localization to the centrosome nor its displacement with the indicated concentration of Ht31, and they do not include data that PKA is displaced from the centrosome with any greater specificity or sensitivity than its displacement from any other subcellular location. Therefore, this statement (as well as the claim in the Abstract that "a specific pool of protein kinase A) (ln15) by the authors is not accurate. The authors should, at the very least, re-word the statement and, for the sake of rigor and support of their hypotheses, confirm that PKA (subunits and/or activity) is displaced from the centrosome.
We thank the reviewer for raising this fair point. We have performed experiments to determine the distribution of PKA (immunofluorescence, using an antibody against PKA Cα). Although the labeling is not very good, we can evidence a slight accumulation of the protein around the centrosome. This enrichment is statistically reduced in the presence of the inhibitory peptide Ht31. This suggest that 1) a pool of PKA accumulates around the centrosome and 2) it is displaced by Ht31.
These results as well as the corresponding images are presented in Figure Supp 7 and described in the new version of the manuscript (lines 236-245).

6. The experiments & results using VCA-centrin-GFP are very intriguing. However, it is crucial that primary data (i.e. photomicrographs/panels of fluorescent images of centrin/VCA-centrin localization, centrosomal F-actin, and roundness) be included for the readers' inspection. Also, it is not clear whether the graphically summarized data on centrosomal F-actin and roundness (Fig. 6b) represent analysis of cells before and after CXCL12 stimulation, or only before or only after. If either of the latter, analysis of these parameters both before and after stimulation should be included.
Representative images of cells expressing centrin/centrin-VCA are now provided and shown in Fig Supp 8. They show that centrin-VCA expressing cells are less deformed (a, b) but also display a higher quantity of F-actin around the centrosome (a).
The effect of stimulation in centrin-VCA expressing cells is now shown in Figure 4e. As mentioned in response to the reviewer #2 (iv), in cells expressing the centrin-VCA construct, the level of actin at the centrosome is higher than in control cells. However, upon chemokine stimulation, the signaling pathways leading to actin reduction are still active so that the level of centrosomal actin decreases (insignificantly different to the control) and the cells do not deform (insignificantly different to the control). These results are now discussed in the manuscript (lines 283-287).

MINOR COMMENTS

1. The writing is generally clear and accurate, but often somewhat 'choppy'. As one of many examples: "As depicted in Figure 1b, in this configuration, we observed that cell deformation starts rapidly after stimulation. The mean delay between cell stimulation and the time when cells start to deform is 112 {plus minus} 10 s (n=48 cells)" could be re-written as "As depicted in Figure 1b, in this configuration, we observed that cell deformation starts rapidly after stimulation, with a mean delay between cell stimulation and initiation of cell deformation of 112 {plus minus} 10 s (n=48 cells)." This is completely stylistic, of course, and would simply (albeit slightly) improve the readability of the work.

We have tried to improve the writing.

2. The authors comment that the contribution of calcium, PI3K, and cAMP signaling "in the early processes allowing the establishment of the asymmetric distribution of cellular components and of the polarity regulators is still elusive" (ln33-35) seems a bit overstated, as there have been numerous, impactful contributions investigating each of those pathways.
We agree that these actors have been already clearly shown to be involved in polarization and/or migration as reported in the review by V. Niggli. However, the precise role they play in the initiation of T cell polarization is not clear. The sentence concerning this point has been modified in the introduction (lines 36-40).

3. The work seems to starts off as being focused on symmetry breaking rather than polarization, but this can be mitigated through rewriting the Introduction.
Symmetry breaking is for us the initial step (prerequisite) for cell polarization. Two sentences have been modified to clarify this point (lines 46-47 and 74-75).

4. The phrase "the major one" (ln47), presumably referring to one of "several local signaling poles" (earlier in ln47) is ambiguous and should be reworded (e.g. "the pole with the highest density of receptors").
The sentence has been modified (lines 53-54).

5. The phrase "variations of cAMP after CXCL12 addition upon dynamic cell imaging" (ln112) is not clear.
The sentence has been modified (lines 124-125).

6. The authors may want to reconsider the use of an ellipsis (ln25), which stands out as somewhat informal for a scientific manuscript.
The sentence has been reworded (lines 27-29).

7. There are several typographical errors throughout that should be addressed (e.g. "AMPc" rather than "cAMP" in the header of Fig7b.; "we were able establish" (ln 130); "while PKA are rapidly activated" (ln133)).
We have corrected typographical errors.

8. The figure legends most often read more like miniature, repeated results sections than detailed descriptions of experimental details and data processing, analysis and depiction.
Figure legends have been rewritten.